SMART GREEN PORTS

LONG TERM ASSESSMENT ENERGY SUPPLY AND DEMAND MODEL

LONG TERM ASSESSMENT ENERGY SUPPLY AND DEMAND MODEL D3.10

GRANT AGREEMENT NO.	101036594
START DATE OF PROJECT	1 October 2021
DURATION OF THE PROJECT	60 months
DELIVERABLE NUMBER	D3.10
TUD	TUD
DISSEMINATION LEVEL	PU
STATUS	V1.0
SUBMISSION DATE	7-7-2026
AUTHOR	Pruyn J. (TUD)

This project has received funding from the European Union's Horizon 2020 research and innovation programme under grant agreement No 101036594.

PU=Public, CO=Confidential, only the members of the consortium (including the Commission Services), CI=Classified, as referred to in Commission Decision 2001/844/EC.

Modification Control

VERSION #	DATE	AUTHOR	ORGANISATION
V0.1	15-04-2025	Pruyn J.	TUD
V0.2	22-01-2026	Wohlleben, D	EWI
V0.3	26-02-2026	Giraldo, J.S	TNO
V0.4	03-05-2026	Lisboa, A.	EDP
V1.0	15-05-2026	Pruyn J.	TUD
V2.0	12-06-2026	Pruyn J.	TUD

Release Approval

NAME	ROLE	DATE
Andre Lisboa	WP Leader	03-05-2026
Reyer Will	Peer reviewer	11-06-2026
Martine Gatsonides	Peer reviewer	05-06-2026
Maarten Flikkema	Scientific coordinator	16-6-2026
Arne-Jan Polman	Project coordinator	7-7-2026

History of Changes

SECTION, PAGE NUMBER	CHANGE MADE	DATE
3.4 (full chapter)	Methodology of EWI Tool	15.01.2026
4.4 (full chapter)	Results of EWI Tool	15.01.2026
3.3 (full chapter)	Methodology of TNO Tool	26-02-2026
4.2 (full chapter)	Results of TNO Tool	26-02-2026
All	Comments addressed	15-05-2026
All	Reviewers Comments addressed	12-06-2026

Table of Contents

Abbreviations

AFOLU	Agriculture, Forestry and Other Land Use
AEL	Alkaline Electorliser
AIS	Automatic Identification System
BAU	Business as Usual
BECCS	Bio-Energy with Carbon Capture and Storage
CBS	Centraal Bureau Statistiek
CII	Carbon Intensity Indicator
CCS	Carbon capture and storage
DACCS	Direct Air Capture and Carbon Storage
DSCPs	Direction-specific connection points
EDP	Energias de Portugal
EEXI	Energy Efficiency Existing Ship Index
EU	European Union
EUR	Eramus University Rotterdam
EWI	Energiewirtschaftliches Institut an der Universität zu Köln (EWI)
GDP	Gross Domestic Product
GHG	Greenhouse Gas
LOHC	Liquid Organic Hydrogen Carriers
LOLP	Loss of Load Probability
IMO	International Maritime Organization
NDCs	Nationally Determined Contributions
MEPC	Marine Environment Protection Committee
PEMEL	proton-exchange-membrane electrolyzers
PtX	Power to X
RES	Regional Energy Strategies
RES	Renewable Energy Sources
SMR	Small Modular Reactor
SSPs	Shared Socioeconomic Pathways
TEU	Twenty-foot Equivalent Unit
WACC	Weighted Average Cost of Capital

WP	Workpackage

Executive Summary

The objective of the WP3 is to deliver a roadmap to develop supply chains: electricity/batteries, hydrogen, ammonia and (Bio-)LNG. The work package encompasses demonstrators linked to BioLNG production and Shore Power applications, with links to demos in WP5 and WP6. And provides input to WP4, WP7, WP8, WP9 and WP10.

This task [T3.6] aims to provide a long-term (2030-2050) assessment of energy demands and supply under various growth scenarios. These models will be used to update the insight of tasks T3.1-3.5. The developed models integrate the effect of new fuels on operations of vessels, trucks and trains, their resulting bunkering strategies and the results identify key infrastructure and fuel acceptance by modalities. These outputs are not only relevant for WP3, but relate also to the work done in WP7 and WP9.

Although in the original planning we planned to go beyond this description and support WP7 and WP8 more directly with assessments of the various MAGPIE Demos, the currently available results of the demos were not suited or relevant to be run through the models. This in a large part due to delays, but also as several demos delivered insights or did not result in direct GHG reductions but served other MAGPIE goals. As result we kept to the original description in the end. This means we focused on a group of models that would address the energy supply chain at various levels of details, which resulted in the overview below.

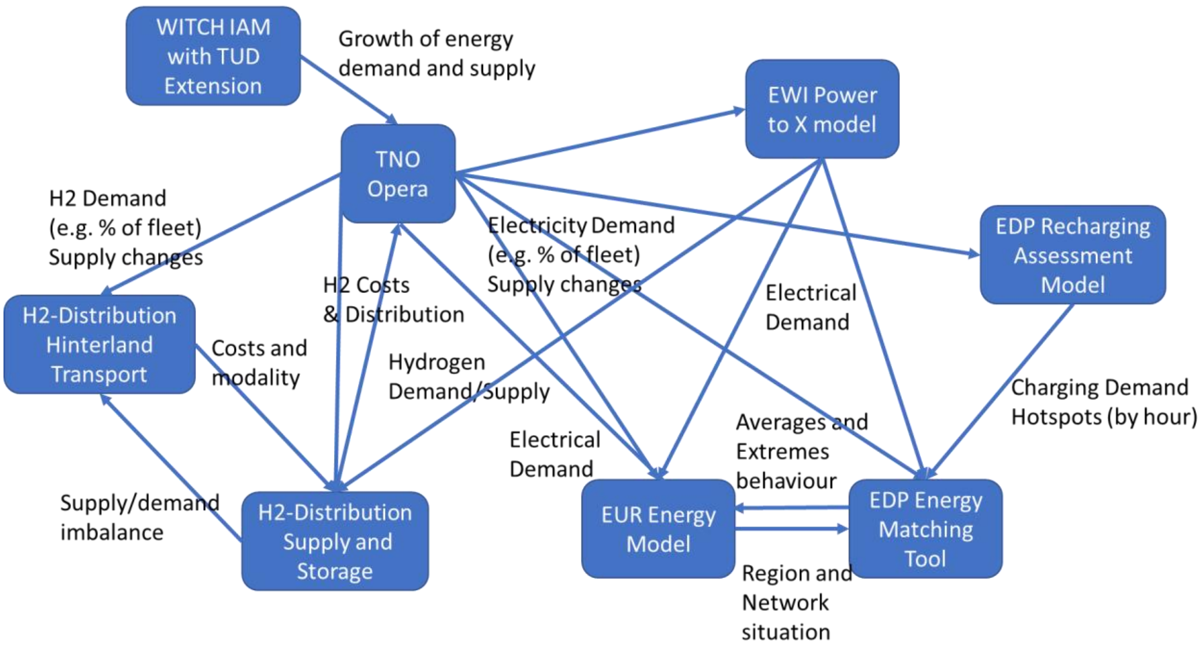

Figure 1: overview of model interactions

In this overview WITCH IAM, an integrated assessment model that covers the global decarbonisation, is the highest level (global and till the end of the century), these results can be used in TNO OPERA, a regional model that identifies energy supply and demand within that region, which focuses on a region and until mid-century. The other models are energy supply chain specific and much more detailed (years to days) and support the insights for each of these supply chains.

The integration/cascading of results was done and led to interesting insights, as shown in part in Chapter 4. A key takeaway for MAGPIE is that, despite the serious downsides of Ammonia as a fuel, the models demonstrate that bio-fuel alternatives will fall short and the import scenarios required to meet the EU energy demand lead to economic stagnation and globally to much higher energy cost levels. In OPERA Nuclear power (SMR) is considered as well, but the input is secondary to import choices and potential and requires quick adaptation to be successful. Furthermore, OPERA confirms that a large industrial complex, like the Port of Rotterdam, would play a key role in energy provision and security.

On the policy level this leads to two important recommendations:

1. To lower the costs of energy and investments in energy, ammonia requires serious consideration, a world of energy without is possible, but again the costs of energy will be far larger than with ammonia as a carrier and fuel.
2. SMR/Nuclear is to be considered (and supported) soon to be relevant based on the model outcomes. As these do not yet include the current global turmoil, energy independence was not yet a key consideration, however, this further strengthens the need for alternative power sources

It should be noted that for ammonia, little is known about the large scale application and the indirect GHG potential. In the past LNG was seen as a key fuel, until methane slip offset the GHG balance in combination with a price shock. Similarly, Ammonia slip could indirectly lead to N_2O forming, leading to additional GHGs in the atmosphere. As not enough is known about the potential slip and counter measures, it is key for Policy to addresses these gaps soon before, like LNG, serious commitments are made.

Finally, the results of T3.6 can be used further in T3.2-T3.5 as well as WP7, WP8 and WP9. As such we see a successful completion of T3.6.

1. Introduction

1.1 Task description

The MAGPIE project is an international collaboration working on demonstrating technical, operational, and procedural energy supply and digital solutions in a living lab environment to stimulate green, smart and integrated multimodal transport and ensure roll-out through the European Green Port of the Future Master Plan and dissemination and exploitation activities. The consortium, coordinated by the Port of Rotterdam, consists of 3 other ports (DeltaPort, Port ofSines and HAROPA Port), 9 research institutes and universities, 32 private companies, and 4 other organisations. The project is divided in 10 main work packages which include energy supply chains, digital tools, 10 demonstrators for maritime, inland water, road, and rail transport, non-technological innovations and the development of a Masterplan for European Green ports.

Aim

The objective of the WP3 is to deliver a roadmap to develop supply chains: electricity/batteries, hydrogen, ammonia and (Bio-)LNG. The work package encompasses demonstrators linked to E-methanol production and Shore Power applications, with links to demos in WP5 and WP6. And provides input to WP4, WP7, WP8, WP9 and WP10.

This task [T3.6] aims to provide a long-term (2030-2050) assessment of energy demands and supply under various growth scenarios. These models will be used to update the insight of tasks T3.1-3.5. The developed models integrate the effect of new fuels on operations of vessels, trucks and trains, their resulting bunkering strategies and the results identify key infrastructure and fuel acceptance by modalities. These outputs are not only relevant for WP3, but relate also to the work done in WP7 and WP9.

1.2 Planning

The task strongly relates to WP7, WP8 and WP9 as indicated in **Fout! Verwijzingsbron niet gevonden.**. It not only integrates the work of Task 3.1-3.5 as indicated in the task description but also relies on consolidated input from the demonstrators (WP8) and non-technological measures (WP7) to generate insights in the future energy supply and demand. This information in turn will be used for WP8 and WP9 to understand the impact of the demonstrators (scale-up, handbook and roadmap). Therefore, the key focus of T3.6 was twofold; alignment of the models on inputs and outputs, especially scenarios and the creation of the in T3.2-T3.5 identified set of key models for this.

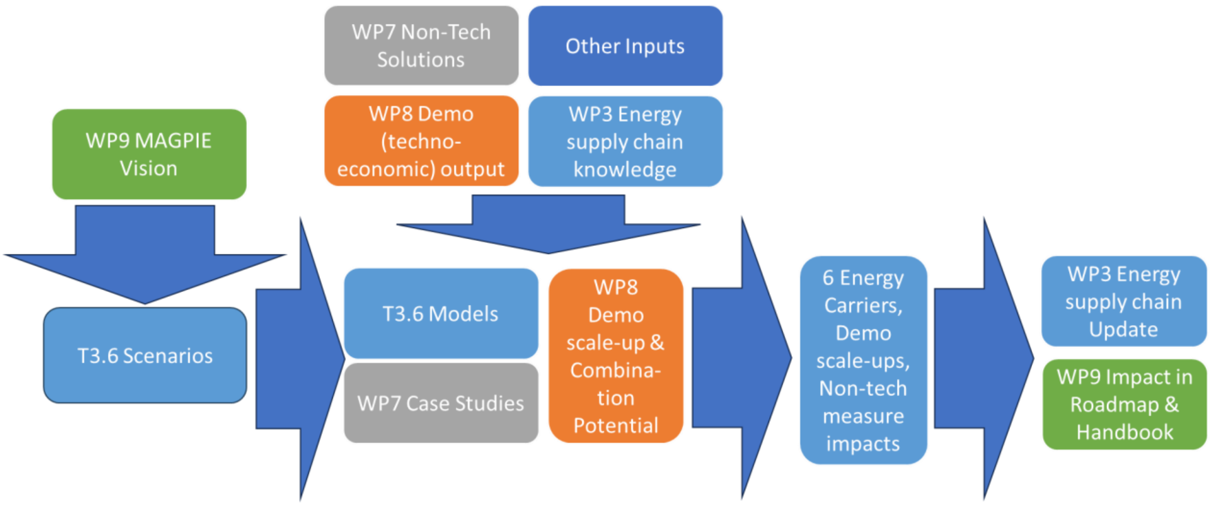

Figure 2: Overview of relation Task 3.6 within WP3 and with WP7-9

As can be seen in **Fout! Verwijzingsbron niet gevonden.** a central role is given to the various demos and solutions within MAGPIE and how to understand their impact on the global energy supply chains and demand. At the start the idea was that this would be a nice extra (as in beyond the scope promised in the GA) to tie in the MAGPIE results more clearly over the WPs and deliver more detailed inputs for the Handbook in WP9 plus support scale-up tasks of WP7 and WP8. Although the original intended combination of models would be suited for this, the delay in demo output prevented a further development along these lines. Nevertheless, any demo can be modelled by at least one model and preferably more.

1.3 Execution

The majority of the planning was carried out as intended, unfortunately, the link with the demos is less strong then originally foreseen. Although discussed in other deliverables (WP8 and demo deliverables from WP3, WP4 and WP5), we identified three issues in this case. Several demos were delayed and adjusted, leading to modelled impacts and results, not requiring further models to build on that. Others focussed more on taking steps towards higher Port Readiness Levels, not directly leading to measurable inputs for models. Finally, two demos (spreading road traffic and the offshore charging buoy) demonstrated the solution to be either not effectively reducing CO2 (spreading road traffic) which is the focus here or not being viable in the Northsea (Charging Bouy). Valid results for a demo, but modelling them made little sense.

This means that the execution is now again in line with the intended work as described by the GA. Therefore, the next chapter (2) will discuss the scenarios created, followed by an overview of the models and a discussion of baseline results in Chapter 4 for the two long term models (the other results can be found in the updates of T3.2-T3.5). Followed by a conclusion on the task in Ch 5.

2. International Scenario Description

A robust way to conceptualize scenario creation is to begin with global pathways and policies, which establish the overall climate and economic context. This can include scenarios aligned with the Shared Socioeconomic Pathways (SSPs), varying from more sustainable worlds to middle-of-the-road trajectories. It can also capture different levels of carbon pricing, from zero or very low carbon taxes to progressively ambitious taxes that escalate over time. Additionally, key global frameworks such as the Paris Agreement targets (e.g., 1.5°C or 2°C by 2100) and Nationally Determined Contributions (NDCs) will heavily influence the boundary conditions. Whether the global community achieves a 1.5°C or 2°C pathway or, conversely, remains on a higher-emissions path will shape the economic and technical feasibility of low-carbon shipping solutions and thus the supply and demand for alternative fuels in ports.

2.1 Main Assumptions

The overarching models in MAGPIE are focussed on achieving a certain goal, allowing certain means and policies to be used to steer the economy in the right direction. It is not intended to understand the impact of 1 solution, but it studies how one solution changes the pathway and choices toward this goal. For this study and in line with the Grant Agreement, we focus specifically on the years 2030, 2040 and 2050 as these are key for the reporting in WP9.

Building on this global backdrop, sectoral policies target the specific mechanisms by which shipping can lower emissions. The International Maritime Organization (IMO) has set various measures to address GHG emissions, including the 2050 target of full decarbonization, the Energy Efficiency Existing Ship Index (EEXI), and the Carbon Intensity Indicator (CII). Modelling the shipping sector under a scenario in which the IMO 2050 target is "on" (i.e., fully binding, leading to deep decarbonization) contrasts sharply with a scenario in which it is "off" or loosely enforced. Moreover, regions can adopt more stringent policies in advance of global agreements, as exemplified by an early introduction of carbon taxes in the European Union. Differences in timing or severity for these policies create alternative paths of technology uptake, such as the need for rapid adoption of zero-carbon fuels or incremental improvements in energy efficiency.

Within this sectoral framework, specific points of variation or "sensitivities" can further refine scenarios. These points might include the level of uptake of alternative fuels—such as ammonia, hydrogen, or biofuels—and the extent to which shipping and other sectors can rely on carbon dioxide removal options (e.g., BECCS or direct air capture) to offset residual emissions. They may also incorporate optimistic or pessimistic assumptions about the decarbonization of the broader energy sector, as electricity-based solutions (for example, in producing e-fuels) become more viable when grids are cleaner, and electricity prices remain stable.

The MAGPIE project introduces demonstrator requirements that take these conceptual scenarios closer to practical application—with a particular focus on ports, which are central to MAGPIE's objectives and strongly interlinked with maritime trade. Demonstrations may explore specific ports, shipping routes, or pilot vessels testing new fuels and operational measures. Incorporating these real-world demonstrations into the scenario framework occurs in the "specific points" phase of scenario creation once the detailed parameters of each are clearly understood. Furthermore, these scenarios should be translated to the port level to assess their implications for port authorities, operations, and infrastructure planning under the varied future possibilities.

2.2 Scenario implementation

In practical scenario development, different combinations of global climate constraints, shipping-specific policies, and fuel-availability assumptions are combined into coherent storylines for maritime decarbonisation. In the present analysis, all scenarios follow the same SSP2 population and GDP projections, so differences in outcomes are driven by policy and technology assumptions rather than by alternative socioeconomic pathways. The scenarios are designed to isolate the main levers that shape shipping transitions in the model: economy-wide climate ambition, sector-specific maritime regulation, and the availability of ammonia as a marine fuel.

For the global pathway, two cases are considered. The BAU scenario represents a continuation of current policy and technology trends without a global climate constraint or additional maritime regulation. It provides the fossil-based reference against which all decarbonisation pathways are compared. The 1.5deg scenario imposes a global carbon budget consistent with limiting end-of-century warming to 1.5 °C. This scenario shows how shipping evolves when the whole energy system is pushed onto a stringent mitigation pathway, including higher carbon prices, lower fossil-fuel use, stronger clean-energy deployment, and tighter cross-sector competition for low-carbon fuels.

On top of these global pathways, additional shipping-specific policy levers are introduced. The 1.5deg-IMO scenario adds a full decarbonisation requirement for shipping by 2050, representing the highest level of ambition aligned with the IMO target. This scenario is useful for assessing what is required to force the maritime sector to decarbonise faster than it would under global mitigation alone. The BAU-MEPC and 1.5deg-MEPC scenarios instead apply the Net-Zero Framework proposed at MEPC-83, with sectoral pricing starting in 2025 under baseline and 1.5 °C conditions, respectively. These scenarios are included to test the effectiveness of an emerging regulatory package that acts directly on shipping, without imposing a hard zero-emission constraint. They are especially informative for observing how fast sectoral policy can trigger fuel switching and emissions reductions relative to broader economy-wide carbon policy.

A separate sensitivity concerns fuel availability. The 1.5deg-NA scenario excludes ammonia from the shipping fuel portfolio. This is not meant to represent a most-likely pathway, but to test the consequences of removing one of the main candidate fuels for long-range maritime transport. The reason for including this case is that ammonia remains controversial because of safety, toxicity, and infrastructure concerns, yet the model results indicate that it is one of the few scalable zero-carbon options for deep-sea shipping. The ammonia-ban scenario therefore helps identify whether the transition depends mainly on climate policy stringency or on access to specific fuel pathways.

Overall, this structured approach—combining macro-scale climate pathways, shipping-specific policies, and detailed points of technological or policy variation—provides a rigorous basis for exploring how international maritime shipping might evolve under different futures and has led to the eight scenarios presented in Table 1. A more detailed discussion of demonstrators and MAGPIE Vision elements that can be implemented, will be given in the next chapters.

Table 1: MAGPIE Main Scenario Overview

Scenario	Global pathway	Shipping taxation (based on MEPC)	Ammonia ban	IMO2050 forced target (zero emission)
Baseline (BAU)	No mitigation, zero carbon tax, 3.5-degree by 2100	No	No	No
1.5-deg	Align with 2-degree scenario by 2100	No	No	No
1.5deg-IMO	Align with 2-degree scenario by 2100	No	No	Yes
1.5deg-NA	Align with 2-degree scenario by 2100	No	Yes	No
Baseline_MEPC	No mitigation, zero carbon tax, 3.5-degree by 2100	Yes	No	No
1.5deg-MEPC	Align with 1.5-degree scenario by 2100	Yes	No	No

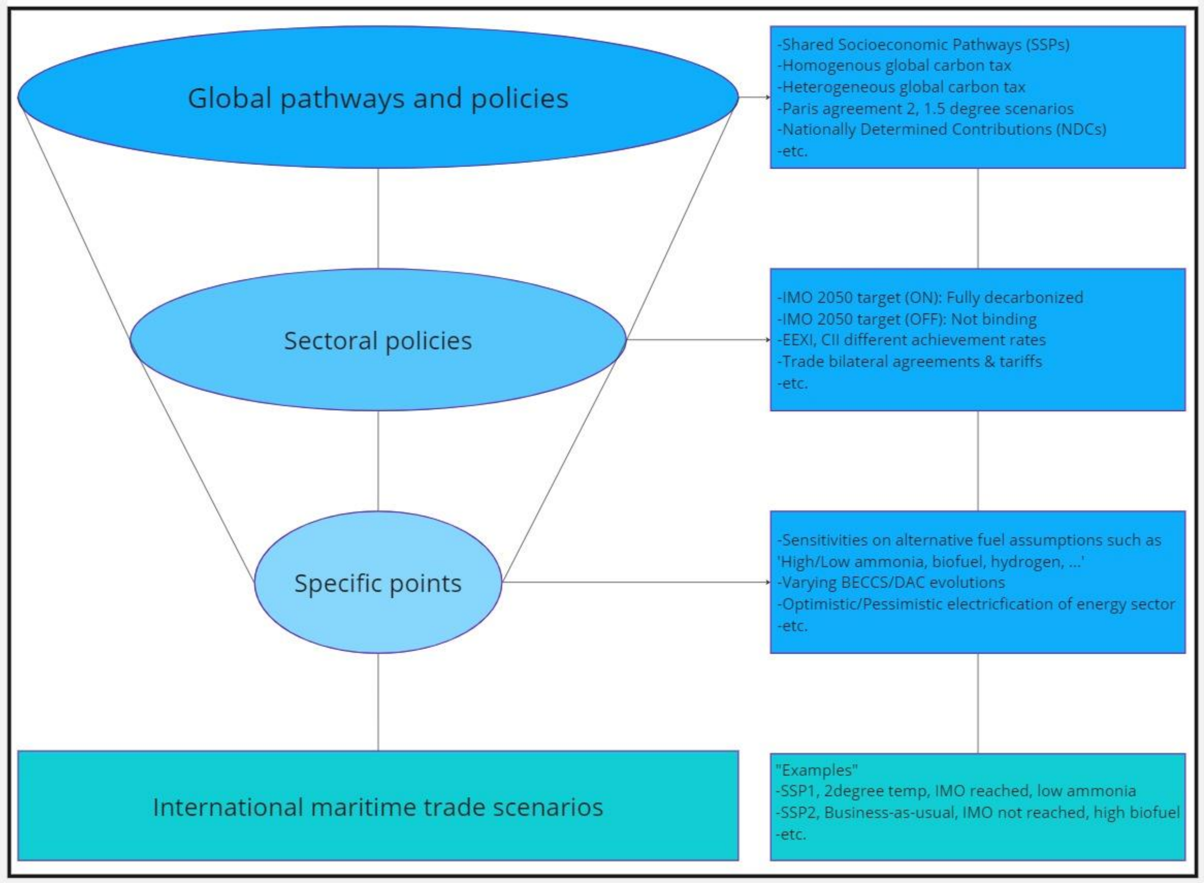

Figure 3: MAGPIE scenario options overview

3. Model descriptions

Based on the scenarios of chapter 2 and the diversity of the demonstrators, it was not possible to develop a single multilevel model. Such a model would be overly complicated and have significant runtimes to allow it to run at the required detail (e..g hourly steps for a period of 50-100 years). As this was realised early on, we decided on a suite of models to address the key questions. These models would link to each other with limited outputs together in order to allow as much consistency as possible but allowing independent development as well. Where possible datasets are directly shared, but as models differ in detail and datasets used originally (e.g. the smallest region in WITCH is Europe, yet OPERA (the model one size smaller) considers a part of the Netherlands). Therefore, in most cases, data needs to be converted to e.g. percentage increase compared to a base year (e.g. 2025 and fractions increased for 2030. 2040 and 2050), so it can be used by the next model. Section 3.1 will discuss the model coverage and interactions, while section 3.2-3.8 will shortly discuss each model, with extensive descriptions available in the Annexes (1-7).

3.1 Scenario implementation

In Figure 4: overview of model interactionsFigure 4, an overview of the seven models developed within T3.6 is given, including their interactions. Although eight elements are presented, the H2-distribution blocks form one model. It should also be noted that there is a certain flow in the model from a global, low detail level to a local, high detail level. This starts with the WITCH AIM extension, which acts globally and flows into the TNO OPERA model which acts nationally/regionally, similar to the H2-distribution model. At the final level we find the local models of EUR, EWI and EDP.

Table 2: Overview of inputs of the models

	Input	Source
WITCH IAM	Scenarios	
OPERA	Regional fuel demand and supply (in % growth)	WITCH IAM
EWI Power to X	E-Fuel Demands (in % growth)	WITCH IAM
H2-model	H2 demand and supply (in % growth)	OPERA
	H2 price trends	EWI Power to X
EUR Energy Model	Electrification Scenario	OPERA

In Table 2, an overview of the input of the models. Further elaboration of outputs is provided in the updates of D3.2-3.5. As can be seen in the table, the combination of WITCH and OPERA provide scenario based inputs to all models that are considered. As there are different assumptions behind models, direct coupling is difficult. E.g. the regions of WITCH IAM are much larger than the region OPERA or EWI Power to X considers, requiring trends to be transferred, rather than absolute values. The same applies for the outputs of OPERA and the Hydrogen pricing of EWI Power to X, these values are of a different detail level again then used by the other models, but trends and knowledge have been shared over the models to achieve the highest consistency.

So, the WITCH AIM and TNO OPERA are the long-term models, while the other models are more short term focussed. As a result, all will be described here, but only for WITCH AIM and TNO OPERA will results be presented in the next chapter (4). For the other models results can be found in the updates of T3.2-T3.5. Also, for WITCH AIM and TNO OPERA additional results are presented in the relevant supply chains.

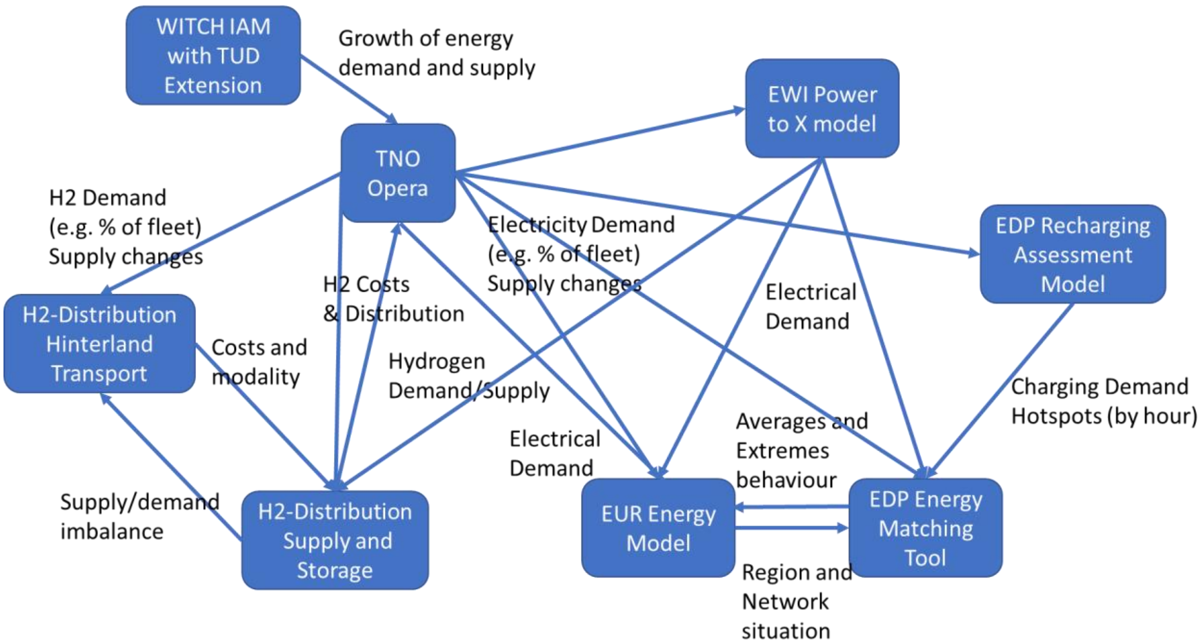

Figure 4: overview of model interactions

3.2 Witch IAM with TUD Extension

Aspect	Description
Space	Global – 17 regions
Time Step	5 years
Era	2020-2100
Carriers	Oil-based fuels, LNG, Biofuels, Methanol, Ammonia, Hydrogen, E-diesel
Objective	Regional least-cost economy optimization
Method	Inter-temporal optimization

Complement to fuel modelling

The core WITCH framework and the representation of hydrogen and hydrogen-based fuels were described in previous deliverables (D3.2 and D3.4). Building on those sections, this subsection focuses on the treatment of incumbent fossil fuels and traditional biofuels, which provide the reference set of energy carriers against which hydrogen-based alternatives compete. In the present application, oil-based fuels, natural gas/LNG, and traditional biofuels are embedded in the standard WITCH representation of non-electric energy demand and primary fuel supply. Their role in the transport system therefore emerges endogenously from relative costs, upstream energy availability, and policy conditions.

In WITCH, fossil fuels and traditional biofuels enter primarily through the non-electric energy branch of the energy system. Non-electric energy demand is represented as a nested structure in which coal and traditional biomass are combined with an aggregate of oil, gas, and traditional biofuels. Within this structure, oil, gas, and traditional biofuels compete as substitutable non-electric energy carriers, so their use is not fixed exogenously but responds to changes in prices, technology, and climate policy. On the supply side, total primary fuel demand is obtained by summing fuel use across sectors. This means that fuel demand from transport is directly connected to fuel use in the rest of the economy. As a result, oil and gas use in shipping-related applications is influenced not only by transport demand itself, but also by cross-sector competition and by the broader regional and global energy balance.

For oil, WITCH includes an explicit extraction module in which production is constrained by available extraction capacity across different resource grades. Extraction capacity evolves over time through investment and depreciation, and extraction costs increase as lower-cost resources are depleted and higher-cost grades are brought into use. This allows oil supply to become more expensive endogenously over time, which is particularly relevant for long-term comparisons between conventional oil-based fuels and alternative low-carbon fuels.

Natural gas is represented more parsimoniously through regional supply curves rather than a separate detailed capacity-expansion module. In practice, regional gas extraction responds to global price signals and regional resource availability, while trade balances the difference between domestic production and consumption. This is important in the present context because natural gas remains relevant both as a direct fuel route, for example through LNG, and as an upstream input to fossil-based hydrogen production routes discussed in D3.4.

Traditional biofuels are represented in WITCH through the traditional biomass and traditional biofuel branches of non-electric energy demand. Their role is therefore more aggregated than that of the hydrogen-based conversion chains introduced in this project. In other words, traditional biofuels are captured as part of the existing non-electric fuel structure, reflecting their contribution as incumbent biomass-derived fuels, but without an explicit detailed conversion chain of the type used for hydrogen, ammonia, methanol, or e-diesel. This is appropriate for long-term system analysis, where the main purpose is to capture their availability and substitution potential rather than detailed process engineering.

Overall, fossil fuels and traditional biofuels in WITCH are represented through a combination of endogenous non-electric fuel substitution, primary resource supply, and regional trade. This provides the benchmark against which hydrogen-based fuels are evaluated in D3.6. Oil-based fuels remain tied to depletion and extraction costs, natural gas depends on regional supply conditions and trade, and traditional biofuels remain part of the pre-existing biomass-based non-electric fuel structure. Together, these incumbent fuel pathways form the reference system from which future fuel shifts in sectors such as road transport, aviation, and maritime shipping can be assessed. Detailed formulation can be found in WITCHmodel(2026) and Naghash(2026).

Shipping activity demand estimation

In the original WITCH framework, international shipping is not represented with enough sectoral detail to analyse future marine fuel competition. Shipping demand is not derived from explicit bilateral seaborne trade flows, cargo composition, or transport work. That is a serious limitation, because maritime fuel use is driven by tonnes moved over distance, not by aggregate economic output alone. In this project, that gap is addressed by introducing a dedicated shipping activity module that links macroeconomic development, trade structure, and maritime transport work within the WITCH framework. The logic is sequential. First, macroeconomic drivers from the model, such as GDP, regional production and consumption, and fuel prices, are used to estimate bilateral trade flows for the main seaborne cargo groups. Second, those bilateral flows are converted into shipping activity by combining traded mass with representative maritime distances between trading regions. This yields transport work in ton-miles, which then serves as the physical basis for vessel allocation, energy demand, and fuel use in the following modelling step. Because the trade module is embedded in WITCH, shipping activity responds consistently to the same socioeconomic and policy assumptions that shape the rest of the energy system.

The trade estimation is based on an extended gravity-model approach. The starting point is the classical gravity intuition that bilateral trade increases with the economic size of origin and destination and decreases with distance:

$$Trade(O,D) \propto \frac{GDP_{Origin} \cdot GDP_{Destination}}{Dis\tan c\, e}$$

This basic relationship is retained but adapted to maritime trade in physical mass units rather than trade value. That distinction is essential here, because emissions and fuel demand depend on transported tonnes and sailing distance. The model distinguishes three broad cargo groups: energy commodities, major bulks, and containerised cargo. This cargo-specific treatment is necessary because the determinants of trade differ across commodity classes and a single generic trade equation performs poorly when applied to all maritime flows together. The selected cargo set covers more than 90% of global seaborne trade.

For **energy cargoes** such as crude oil and petroleum products, natural gas, and coal, bilateral trade is estimated using a log-log specification with origin-destination fixed effects

$$\ln T\,rade(O,D,t) = \beta_0 + \beta_1 \ln V_1 + \beta_2 \ln V_2 + \cdots + \beta_n \ln V_n + \lambda_{OD}$$

where $TradeOD{,}t$ is bilateral trade from origin to destination in year t, Vn denotes the selected explanatory variables, βn are the corresponding elasticities, and $\lambda\ OD$ captures persistent bilateral trade structure. The explanatory variables include GDP, production, and consumption of exporter and importer regions, together with distance and bunker-fuel prices. This allows the model to capture not only economic scale, but also regional supply-demand balances and persistent trading relationships. That is important for shipping because energy commodities often show strong bilateral trade habits and can exhibit cross-trading, where a region both imports and exports the same commodity.

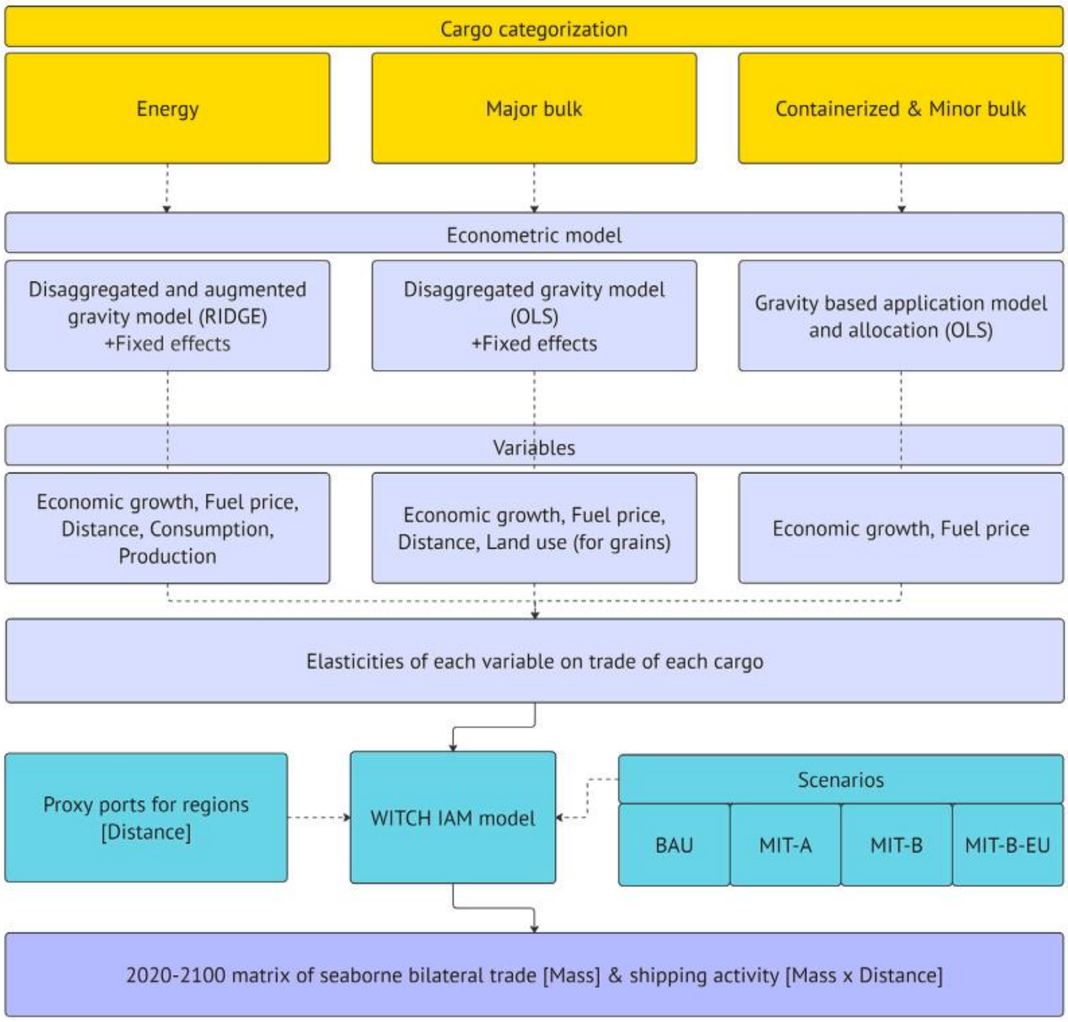

Figure 5: WITCH model extension overview

For **major bulk cargoes**, particularly grains and iron ore, the same gravity logic is used, but with a simpler determinant structure to avoid double-counting the effect of economic growth. Since production and consumption of these bulk commodities are already strongly shaped by GDP, the projection model relies mainly on exporter and importer GDP, distance, and fuel prices. For grains, agricultural land use in the exporting region is added as an additional explanatory variable to better capture physical production capacity. This gives a cargo-specific specification that remains consistent with the broader gravity framework while reflecting the different economic drivers of bulk trade.

For **containerised cargo**, a different approach is used because historical data are often available in regional aggregates and product value rather than in detailed bilateral mass flows. The first equation estimates aggregate import or export demand as a function of GDP and fuel prices:

$$Trade_{X\ or\ I}(t, O\ or\ D) = \beta 0_{X\ or\ I} \times GDP_{X\ or\ I}^{\beta 1} \times fprice_{X\ or\ I}^{\beta 2}$$

$$Trade_{OD,t} = Import_D(t0) \times \exp\left(\beta 1_I .\ \ln\left(\frac{GDP_D(t)}{GDP_D(t_0)}\right) + \beta 2_I .\ \ln\left(\frac{fprice(t)}{fprice(t0)}\right)\right) \times \frac{Allocation_O(t)}{\sum_O Allocation_O(t)} Allocation_O(t) = \beta 0_X \times GDP^{\beta 1x}(t) \times fprice^{\beta 2x}(t)$$

This two-step structure first projects the scale of regional container trade and then distributes it bilaterally across origins. It is less data-intensive than a full bilateral mass model and better suited to the characteristics of containerised trade data.

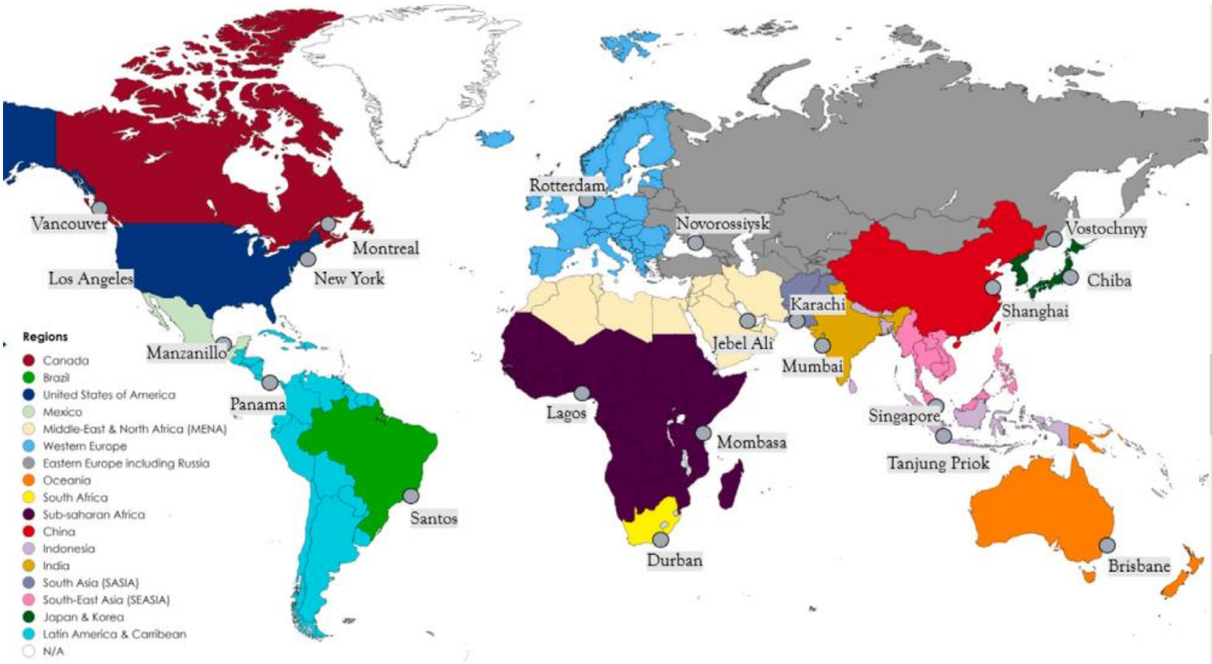

Figure 6: WITCH IAM regional devision overview

Once bilateral trade has been estimated in tonnes, it is converted into **shipping activity demand** using representative maritime distances. This step is more than a simple region-to-region centroid approximation. The model assigns one or more **proxy ports** to each region, calculates average maritime distances between those proxy ports, and uses those distances to derive transport work in ton-miles. The explicit purpose is to represent the seaborne portion of trade rather than total trade by all transport modes. For adjacent regions where land transport or pipelines account for a large share of flows, such as Russia-China or Canada-USA, only the seaborne component is retained. This avoids overstating maritime demand in cases where physical trade exists but does not primarily move by sea.

The distance estimation is also adjusted to remain physically plausible for global shipping. Representative sea routes are used rather than straight-line distances, and major geographic chokepoints are taken into account. In the integrated shipping application, routing also respects relevant vessel-size restrictions where needed to preserve realistic long-haul patterns. This matters because distance is not just a geometric input; it shapes transport cost, ton-mile demand, and ultimately fuel use. A poor distance approximation would contaminate the whole chain from trade estimation to energy demand.

The result of this module is a set of cargo-specific bilateral shipping activity projections in ton-miles that evolve endogenously with GDP, trade patterns, fuel prices, and climate policy. This is the key bridge between the macroeconomic world of WITCH and the physical world of maritime transport. It ensures that later estimates of vessel deployment, fuel consumption, and emissions are grounded in scenario-consistent transport work rather than imposed exogenously. The next subsection uses this shipping activity output to derive energy demand and fuel requirements.

Converting activity to energy requirement

Once bilateral shipping activity has been estimated in ton-miles, it must be translated into physical energy demand. This step is necessary because shipping emissions and fuel requirements are determined not only by transport work, but also by the type, size, and operational performance of the vessels providing that transport. A given level of ton-mile demand can therefore imply very different energy requirements depending on whether it is served by small regional ships or by large long-haul vessels. In the WITCH-TUD extension, this conversion is carried out through a bottom-up shipping-energy module that links transport activity to ship classes, vessel productivity, and fuel intensity.

The logic is straightforward. First, traded cargoes are mapped to the main vessel classes used in maritime transport. Tankers are used for oil, oil products, LNG, and hydrogen-related liquid cargoes; bulk carriers are used for iron ore, grains, and minor bulks; and container ships are used for containerised cargo. Second, the estimated shipping activity is distributed across vessel size categories within each ship class. Third, average fuel consumption and productivity values are applied to convert the allocated activity into energy demand. This structure allows the model to reflect the fact that large vessels are generally more energy-efficient per ton-mile than smaller vessels, while still preserving the heterogeneity of the fleet. To ensure consistency, vessels are grouped into four size categories: small, medium, large, and ultra-large. These categories are defined separately for tankers, bulk carriers, and containerships using deadweight tonnage, and for containerships also linked to TEU classes. This aggregation reduces the dimensionality of the model while retaining the main operational differences that matter for energy use. The size structure is important because fuel consumption, cargo productivity, and shipbuilding costs all vary systematically with vessel size. The allocation of shipping activity to vessel sizes is based on observed route patterns rather than on a fixed or purely theoretical rule. Using AIS-based shipping data, routes are classified jointly by distance and demand level. Demand is divided into quartiles, while distance is grouped into six ranges, from short-haul regional routes to ultra-long-haul intercontinental trades. For each vessel type, the observed distribution of ship sizes within each distance-demand block is used to derive size shares. These shares are then applied to projected shipping activity. This approach is more realistic than assigning one vessel size per route, because actual shipping routes are served by a mix of ship sizes, and that mix evolves systematically with route length and demand scale. The core allocation equation is:

$$mtrade(O,D,t,ss) = Trade(O,D,t) \times p(jship,q,d,ss)$$

where $Trade$ is the traded cargo flow, $mtrade$ is the portion allocated to vessel size class ss, and $p(jship,q,d,ss)$ is the empirically derived size share for ship type $jship$ in the corresponding demand quartile q and distance category d. In practice, this means that short-distance and low-volume trades are assigned a larger share of small and medium vessels, while long-distance and high-volume corridors receive a larger share of large and ultra-large ships. This observed shift toward larger ships on longer and denser routes is consistent across tankers, bulk carriers, and containerships.

Once activity is allocated to vessel types and sizes, the model converts this activity into energy demand using two physical parameters: **fuel consumption intensity** and **productivity**. Fuel consumption intensity is measured in energy per ton-mile and reflects how much energy a vessel consumes to move one tonne of cargo over one nautical mile. Productivity is measured in ton-miles per unit of ship capacity and year and captures how intensively a vessel type and size is used in practice. These parameters are derived from operational evidence, primarily from the IMO Fourth GHG Study, and then aggregated to the ship-size classes used in the model. The energy requirement of shipping is then calculated as:

$$EN_{t,n} = \sum_{jship} FC_{jship,t,n} \times \Pr o\, ductivity_{jship,t,n} \times Kship_{jship,t,n}$$

where ENt,n is total shipping energy demand, FC is fuel consumption intensity, $Productivity$ is vessel productivity, and $Kship$ is the active fleet capacity required to satisfy shipping demand. This equation provides the link between shipping activity and final energy use: more transport work requires either more active fleet capacity or more intensive use of existing ships, and the resulting energy demand depends on the efficiency of the corresponding vessel categories. The required active fleet capacity is obtained from shipping activity and vessel productivity:

$$Kship_{jship,t,n} = \frac{\sum_{cc \in mapped\ to\ jship}^{S} hipping\ \ Demand_{cc,t,n}}{\Pr o\, ductivity_{jship,t,n}}$$

This formulation makes productivity a central parameter. If ships are more productive, meaning they deliver more ton-miles per unit of capacity each year, less fleet capacity is needed to satisfy a given transport demand. Conversely, lower productivity implies a larger active fleet and therefore higher associated capital requirements. Even though the main purpose of this subsection is energy estimation, this fleet-capacity link is important because it connects energy demand to fleet evolution and, later, to shipbuilding investment.

Fuel consumption intensity is also differentiated by ship type and size. The empirical results reported in the underlying study show a clear and expected pattern: fuel consumption per ton-mile declines as vessel size increases. Bulk carriers are the most energy-efficient among the three main ship types, while container ships have the highest energy use per ton-mile due to their higher service speeds and more demanding operating profiles. Tankers lie in between, with strong variation across size classes. This pattern reflects the economies of scale of large ships and is important for scenario analysis, because a shift in trade structure can change average fleet efficiency even before any fuel switching occurs.

The same applies to productivity. Productivity values are calculated for each vessel type and size group using observed operational data and then aggregated into the model's four size classes. This allows the model to capture the fact that large ships are not only more efficient in fuel use per ton-mile, but also often deliver more transport work per unit of installed capacity. The combined effect of size-dependent fuel intensity and size-dependent productivity is therefore a key driver of future shipping energy demand.

In practical terms, this module converts macroeconomically driven trade flows into a physically grounded estimate of shipping energy demand. Because the previous step already provides bilateral ton-mile activity by cargo type and region pair, and because the current step maps that activity onto observed vessel structures, the resulting energy requirement remains consistent with both the global scenario assumptions and real shipping operations. This is one of the main strengths of the WITCH-TUD extension: energy demand is not imposed by an external intensity factor, but emerges from the interaction between trade patterns, route structures, vessel deployment, and fleet performance.

This energy-demand estimate then becomes the basis for the next stage of the model, in which fuel competition is introduced. Once the total energy requirement is known, the model can allocate that demand across oil-based fuels, LNG, biofuels, hydrogen, ammonia, methanol, and e-diesel according to the technology and policy conditions of each scenario.

Other parts of the model

A few additional elements complete the WITCH-TUD framework and help explain how the different modules interact. Cargo groups are first linked to the main vessel classes in a physically consistent way: energy commodities are assigned to tankers, major bulks to bulk carriers, and containerised goods to containerships. Each vessel class is then further split into size groups using AIS-based evidence on route distance and demand. This matters because vessel productivity, fuel intensity, and capital costs vary systematically by ship type and size, so the same ton-mile demand can imply different fleet and energy requirements.

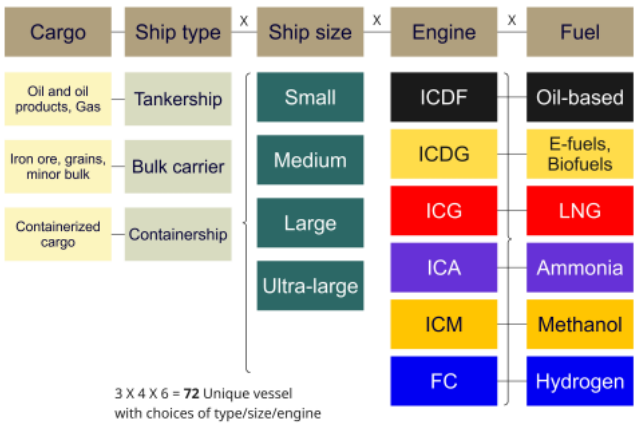

Figure 7: Ship type categorizations

The model also distinguishes the main propulsion options across fuels. Oil-based fuels, biofuels, and e-diesel are assumed to use conventional diesel engines, while ammonia, methanol, and natural gas require modified combustion systems. Hydrogen is represented through fuel-cell propulsion. These differences affect vessel-side economics because alternative fuels are associated with different engine, storage, and onboard-system requirements. As a result, fuel competition is shaped not only by upstream fuel costs but also by differences in ship technology and retrofit or newbuilding costs.

In addition, a gradual exogenous improvement in ship energy efficiency is included over time. This means that future shipping energy demand depends not only on activity growth and fuel switching, but also on ongoing technical progress in vessel performance. The model therefore captures both structural change in the fuel mix and background improvements in operational efficiency.

Finally, the shipping module remains embedded in the broader WITCH climate framework. Maritime fuel choices are evaluated under the same economy-wide climate constraints as the rest of the energy system, including global carbon budgets and endogenous carbon prices. This is important because shipping is not treated in isolation: its fuel demand feeds back into electricity, hydrogen, biomass, and carbon-use requirements, while competition from other sectors affects the cost and availability of these fuels. In this way, the model preserves consistency between shipping decarbonisation and the wider energy transition. More details of model description can be found in Naghash(2026). The regional demand output for the EU in all scenarios is transferred to TNO as this is a complex process it will be discussed in detail next.

3.3 Downscaling and soft-linking to the national model

Aspect	Description
Approach	Feed-forward soft-link (one-way)
Spatial scope	West-Europe (TU Delft/WITCH) → Netherlands (OPERA) → Port of Rotterdam
Time horizon	2030, 2040, 2050
Carriers	Oil, Traditional biofuels, LNG, Methanol, Ammonia, Hydrogen, e-fuels
Link direction	TU Delft → Translation Layer → OPERA (feasibility + effective price read-back)
Downscaling factor α	0.240 (Rotterdam share of West-Europe bunker energy, calibrated on 2020 data)

The WITCH–TU Delft shipping model provides a globally consistent picture of how seaborne trade, fleet composition and fuel use evolve under different climate and policy assumptions. However, it operates at the West-Europe regional level and does not resolve constraints specific to an individual port or national energy system. Conversely, TNO's OPERA model captures the Dutch energy system in high spatial and sectoral detail but does not endogenously model global fleet behaviour or international marine fuel markets. In earlier OPERA-based work, marine fuel shares for seagoing vessels were imposed as exogenous bounds rather than derived from an explicit fleet model.

Coupling the two models addresses this gap. TU Delft provides scenario-consistent global fuel dynamics; OPERA tests whether those dynamics are feasible given national supply availability, infrastructure limits and policy obligations. The coupling is implemented as a feed-forward soft-link: WITCH–TU Delft outputs drive Rotterdam-level fuel demand and mix, and OPERA checks feasibility and returns effective prices (willingness-to-pay) for each fuel under the ADAPT and TRANSFORM scenarios. Table 4 summarises the capabilities added by coupling relative to each standalone model.

Table 3: Comparison of the WITCH-TU Delft model, standalone OPERA, and the coupled framework

Dimension	WITCH-TU Delft (upstream)	OPERA standalone (previous)	Coupled framework (this work)
Spatial resolution	Global / 17 regions	Netherlands + Port of Rotterdam sub-regions	Port of Rotterdam (proportional downscaling)
Marine fuel shares	Endogenous fleet optimisation	Exogenous bounds (previous approach)	TU Delft shares enter OPERA as fixed bounds
Port-level detail	None	Single distribution key	α calibration + vessel-segment disaggregation
Key output	West-Europe fuel mix by scenario	National fuel cost and supply mix	Port fuel demand, domestic/import split, WTP curves

A proportional downscaling approach (van Vuuren et al., 2007) translates West-Europe fuel demand totals to the Port of Rotterdam. A single allocation factor α is calibrated on Port of Rotterdam bunker sales for 2020 and held constant across all scenarios and years, ensuring that differences in port-level outcomes between scenarios reflect the upstream assumptions rather than the scaling method.

Calibration of α. Rotterdam bunker sales for 2020 total 373.9 PJ (LHV basis) (Havenbedrijf Rotterdam N.V., 2025). Total West-Europe sea-going shipping energy in the WITCH Baseline for 2020 is 1,556.6 PJ (1.557 EJ). The allocation factor is therefore:

$$\alpha \;=\; E\_Rotterdam, 2020 \;/\; E\_WITCH, Baseline, 2020 \;=\; 0.374\,EJ \;/\; 1.557\,EJ \;=\; 0.240$$

For each scenario s, year y and fuel f, Rotterdam bunker energy is then:

$$E\_ROT(s, y, f) \;=\; \alpha \;\times\; E\_WE(s, y, f)$$

Because α is identical for all fuels, Rotterdam fuel shares are equal to the West-Europe fuel shares from WITCH-TU Delft. Vessel-segment disaggregation is carried out in a second step using TU Delft EuropeFleet deadweight-tonnage data as allocation weights, distributing Rotterdam fuel totals across bulk carriers, container ships and tankers for each scenario-year. Three consistency checks (fuel mass balance, weight normalisation per engine class, share preservation) confirm internal consistency after each run.

Four policy-relevant scenario bundles are constructed: ADAPT + FuelEU, TRANSFORM + FuelEU, ADAPT + IMO MEPC 83, and TRANSFORM + IMO MEPC 83. The ADAPT bundle maps to the baseline-oriented TU Delft variants (Baseline-MEPC, base-FuelEU); TRANSFORM maps to the 1.5 °C variants (1.5-MEPC, 1.5-FuelEU).

Port-level fuel mix results (2020-2050)

Figures 5-8 show the Rotterdam-downscaled fuel mix for all four scenario bundles. Under the ADAPT pathway (Figures 5 and 7), traditional biofuels (trbiofuel) progressively replace fuel oil after 2030, reaching approximately 379 PJ (FuelEU) and 359 PJ (MEPC) by 2050, with total demand around 523 PJ. Under the TRANSFORM pathway (Figures 6 and 8), ammonia dominates by 2050 (≈ 300–318 PJ), with total demand around 402–403 PJ. Note: 'trbiofuel' =

traditional biofuels (HVO, FAME, Annex IX B feedstocks); 'rhc' = renewable hydrocarbon e-fuels.

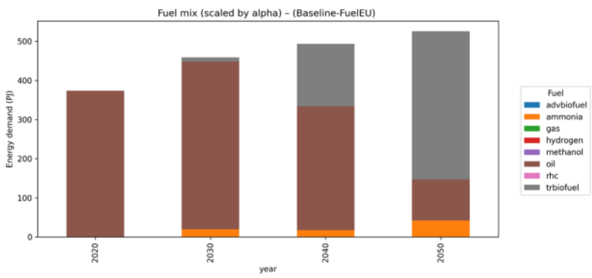

Figure 8: Fuel mix under FuelEU × ADAPT Source: Landsmeer (2026)

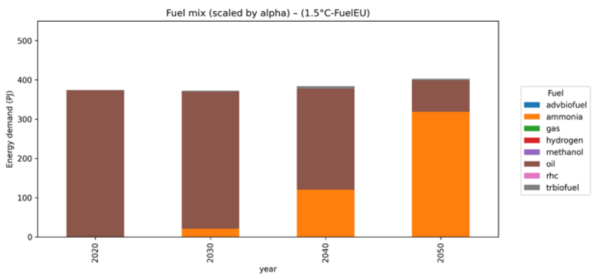

Figure 9: Fuel mix under FuelEU × TRANSFORM. Source: Landsmeer (2026)

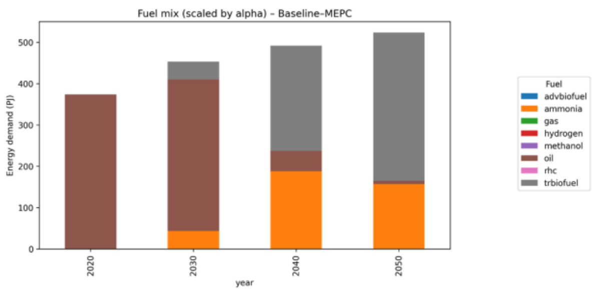

Figure 10: Fuel mix under MEPC × ADAPT Source: Landsmeer (2026)

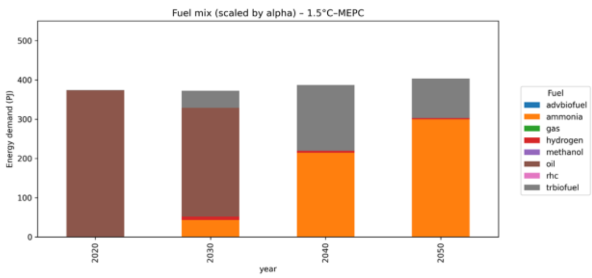

Figure 11: Fuel mix under MEPC × TRANSFORM. MEPC induces faster fuel oil phase-out; hydrogen appears in the TRANSFORM–MEPC mix in 2030–2040. Source: Landsmeer (2026)

Feed-forward soft-link and translation layer

The Rotterdam-downscaled dataset is passed to OPERA via a translation layer. Downscaled TU Delft fuel demand targets enter OPERA as fixed boundary conditions; OPERA outputs are read only to check feasibility and derive effective prices. The translation layer carries out four tasks:

1. Unit alignment: all energy values are expressed in PJ per year on an LHV basis.
2. Category mapping: TU Delft vessel segments are linked to OPERA technology lines by engine class and fuel type using a fixed concordance table.
3. Time alignment: only the 2030, 2040 and 2050 snapshots are used; no interpolation or extrapolation is applied.
4. Policy cost separation: GHG-intensity requirements are embedded in the upstream TU Delft fuel shares and are not re-imposed in OPERA, preventing double counting.

Direction-specific connection points (DSCPs) are defined for each variable exchanged between models (Krook-Riekkola et al., 2017). Table 4 lists the six DSCPs.

Table 4: Direction-specific connection points (DSCPs) in the WITCH-TU Delft / OPERA soft-link. Each DSCP specifies direction, variable, unit, mapping rule and notes to prevent double counting and unit drift

#	Direction	Variable	Unit	Mapping rule	Notes
1	TU Delft→OPERA	Bunker energy, maritime shipping (2030/2040/2050)	PJ/y	Direct (unit check)	Segment = maritime ships
2	TU Delft→OPERA	Fleet fuel share, maritime shipping	% per fuel	Upper/lower bound (±Δ)	Applied as target bounds per fuel f
3	TL→OPERA	Import availability cap per fuel/year	PJ/y	Cap value	Applied where data are available
4	OPERA→TL	Binding national caps / first-year availability	PJ/y	Constraint set	Used for minimal feasibility adjustments
5	OPERA→TL	Domestic-vs-import split per fuel/year	PJ/y, %	Read volumes by origin	Used for WTP curves and infrastructure analysis
6	OPERA→TL	Effective price (shadow price diagnostic)	M€/PJ	Marginal value via small import test	Diagnostic only; drives WTP curve construction

Where OPERA cannot find a feasible solution for a given scenario-year, a minimal import volume is introduced for the constrained fuel. The effective price for each fuel (input price + shadow price) is then read from the OPERA output. When no supply or emission constraint binds, the effective price approximates the exogenous input price; when a constraint binds, the shadow price rises and signals scarcity.

Key output: willingness-to-pay curves and domestic-import attribution

WTP curves are constructed by running OPERA repeatedly with incrementally relaxed import limits, one fuel at a time. Figures 4 and 5 show the WTP curves for biodiesel and ammonia under the FuelEU and MEPC frameworks respectively, across all scenario-year combinations.

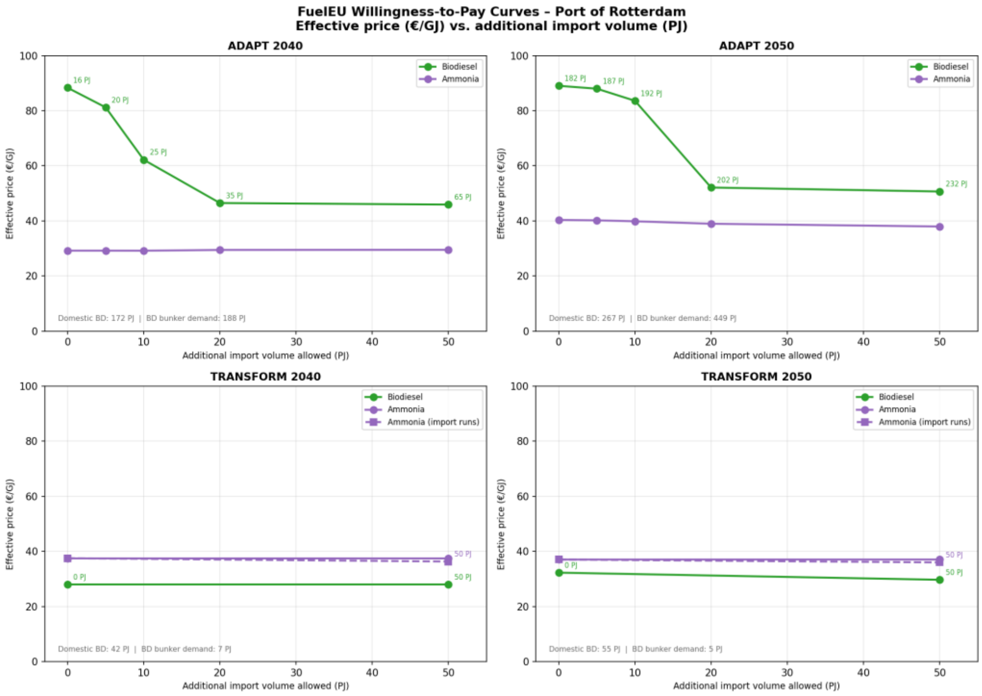

Figure 12: Willingness-to-pay (WTP) curves for biodiesel and ammonia under the FuelEU policy framework, derived from national OPERA runs (Rotterdam ≈ 85 % of national values). Effective price (€/GJ) is plotted against additional import volume (PJ) above the minimum-feasibility baseline. Annotations show total biodiesel import volume at each run point. Source: Landsmeer (2026)

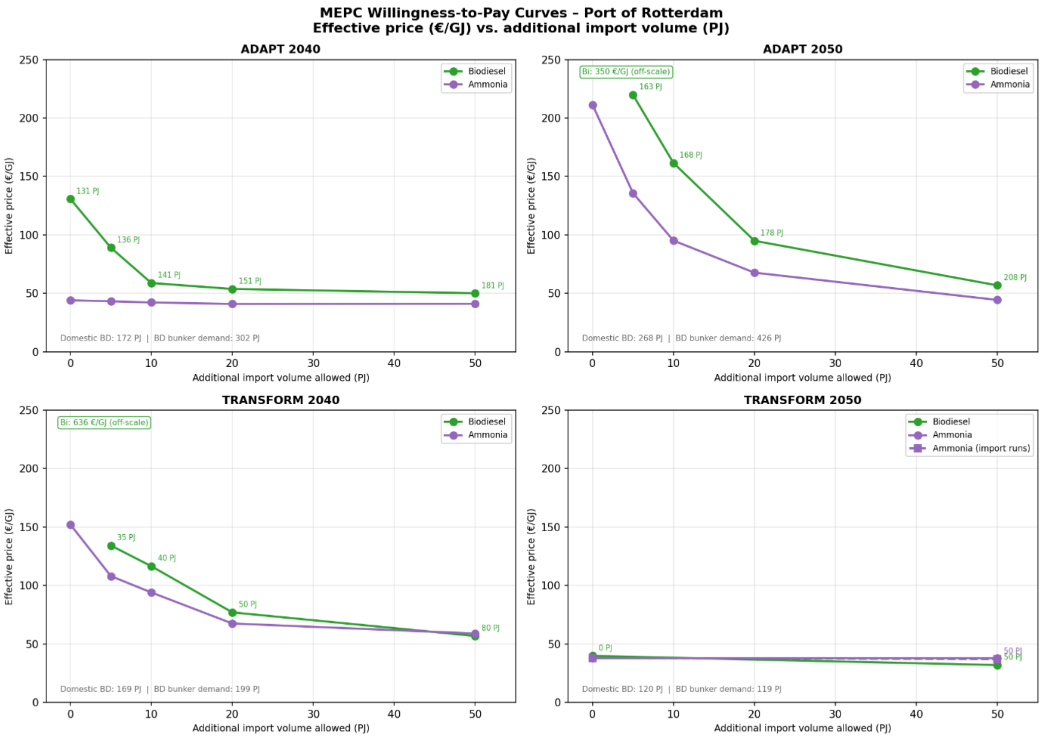

Figure 13: Willingness-to-pay (WTP) curves for biodiesel and ammonia under the MEPC policy framework, derived from national OPERA runs (Rotterdam ≈ 85 % of national values). The y-axis is scaled to 250 €/GJ; off-scale values are annotated within the panel. Source: Landsmeer (2026)

Three findings are consistent across both policy frameworks. First, under ADAPT scenarios the biodiesel supply constraint is binding: domestic availability falls short of demand, with minimum import requirements ranging from 16 PJ (ADAPT-FuelEU 2040) to 182 PJ (ADAPT-FuelEU 2050) nationally; Rotterdam-level values are approximately 85 % of these. Second, ammonia demand is fully covered by domestic production in all scenarios; no import is required to meet feasibility. Third, under TRANSFORM, both fuels trade close to their input prices in 2050, indicating that the 1.5 °C pathway eliminates the scarcity premium through earlier and stronger shifts to zero-carbon fuels.

The biofuel volumes implied by the ADAPT scenarios are substantial relative to European supply: at approximately 359–379 PJ for Rotterdam alone, they correspond to 8.6–9.0 Mtoe, or 14–25 % of total sustainable biomass availability for traditional biofuels across the entire EU (WGMM, 2026). These results should therefore be interpreted as upper-bound signals from the top-down model rather than as feasible supply outcomes, and they point directly to the import infrastructure requirements assessed further in the MAGPIE infrastructure analysis.

Further detail on methodology, results, sensitivity analysis and infrastructure implications is provided in Landsmeer (2026).

3.4 TNO Opera National Model

The OPERA model is an optimization model focused on minimizing the societal costs of the Dutch energy system (van Stralen, 2021). Part of these costs are associated with the fuels used to fulfil the consumption requirements of the system. Although OPERA shares the same general goal as WITCH, their methodologies have significant differences. Contrary to the global vision of the former, the latter focus on a national level. By geographically zooming in, different considerations come into play, namely all those that are particular to the country under analysis. Therefore, and in line with the objectives of the MAGPIE project, OPERA searches for an optimal fuel mix portfolio for the transport sector. The model uses insightful information from the WITCH model to define boundary conditions concerning oil-based fuels, LNG, biofuels, hydrogen, ammonia, methanol, aligned to specific national scenarios.

Aspect	Description
Space	National (7 offshore regions and 13 onshore representing the Netherlands)
Time Step	Hourly resolution for one horizon year
Era	2030-2050 in 5-year intervals
Carriers	Electricity, Hydrogen, Methane, Biomass, Biogas, Heat, Diesel, Gasoline, Kerosene, Synthetic Fuels, Coal, Lignite, Heating Oil, LPG, Biodiesel, Bioethanol, Methanol, Ammonia, Synthetic Methane, District Cooling
Objective	Minimizing the societal costs of the Dutch integrated energy system
Method	Optimization model

By zooming in geographically, different considerations come into play, namely those particular to the country under analysis. A very specific but illustrative example relates to natural gas pipelines that can be retrofitted to transport hydrogen. Their availability might reduce overall system costs, thereby positioning hydrogen as a central player in the transition pathway. Thanks to OPERA, a model that uses distribution and transmission networks to couple supply and demand, this type of assessment is possible. On the other hand, OPERA has high time resolution. As a model oriented to national planning, it is important to ensure that supply and demand are constantly in balance. By doing so, it is also possible to capture and integrate their variability along the pre-defined time-horizon.

OPERA allows the regionalization of the nation under analysis. This does not mean that the optimization is carried out per region. Instead, it means that a regional analysis of the national optimization results can be performed. In the MAGPIE project, the Rotterdam Area, including the port of Rotterdam, was divided into several sub-regions, and the rest of the Netherlands has a coarser representation. In particular, the model distinguishes 13 onshore and 7 offshore regions. The onshore regions include the new Port of Rotterdam sub-regions (Botlek, Europoort, Groot-Rotterdam, Maasvlakte, Moerdijk, and Pernis), and the previous default regions, including South Holland remaining, Limburg, Mid NL, North Brabant remaining, North Holland, North NL, and Zeeland. Offshore regions represent distinct offshore wind hubs. The new regionalization is illustrated in Figure 14.

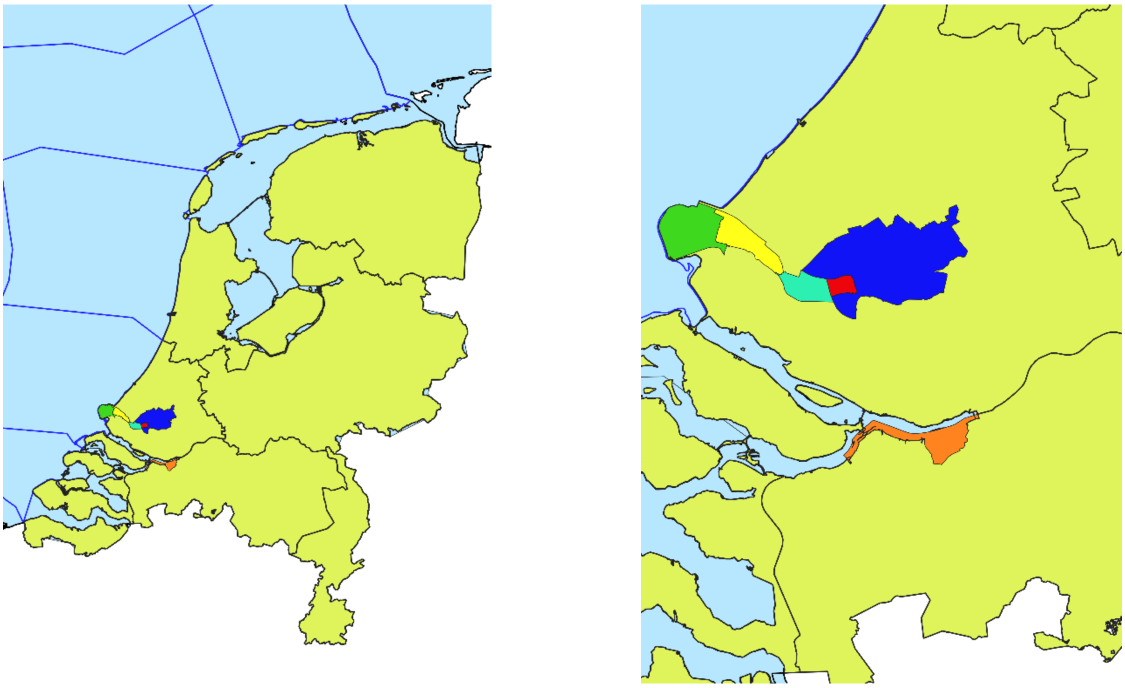

Figure 15: Regions in OPERA and new regions for the Port of Rotterdam area

Regionalisation

Regionalisation uses distribution keys to disaggregate national inputs into regional values while maintaining national totals. Each variable, for example, energy demand, renewable resource potential, or technology availability, is split across regions so the shares sum to one. This preserves aggregate balances and captures spatial diversity in energy use and supply.

Model input data, such as sectoral service demand and renewable resource potentials, are specified at the national level and allocated to regions and sub-regions using a dimensionless distribution key system. These keys assign regional shares to national totals and can be applied to demands, energy carriers, conversion technologies, and aggregated sectoral groupings within the model.

Three main distribution key types are used:

1. **Industry-based keys:** Plant-level CO_2 emissions from the MIDDEN database are used as an indicator of industrial activity (PBL Netherlands Environmental Assessment Agency, n.d.). Assuming emissions are proportional to production volumes, industrial energy and feedstock demands are allocated spatially according to the observed emissions pattern.
2. **Population-based keys:** Population statistics from Statistics Netherlands (CBS) are used to allocate demand for households, services, and passenger transport, and to inform the spatial suitability of related technologies (Statistics Netherlands, 2025).
3. **RES-based keys:** Data from the Regional Energy Strategies (RES) are used to distribute solar, wind, and geothermal potentials, as well as planned deployments, across locations.

In addition, a fourth, case-specific category is applied when dedicated spatial information is required (e.g., allocating aviation demand to airports, navigation demand to ports, and waste incineration to waste treatment hubs). Table 5: Baseline population-based regional distribution based on CBS population distribution data (2024) (Statistics Netherlands, 2025) shows the baseline population-based distribution derived from Statistics Netherlands (CBS) population data (Statistics Netherlands, 2025). This allocation serves as the default spatial split in OPERA, unless it is replaced by emission-based industry keys or sector-specific distribution assumptions. Notice that within the Port region, only Groot-Rotterdam is assumed to have population, since the other subregions are mostly industrial.

Table 5: Baseline population-based regional distribution based on CBS population distribution data (2024) (Statistics Netherlands, 2025)

Region	Default distribution key
Port of Rotterdam	
Groot-Rotterdam	8%
Rest of NL	
South Holland remaining	14%
Limburg	7%
Mid NL	29%
North Brabant remaining	14%
North Holland	16%
North NL	10%
Zeeland	2%

To allocate industrial energy demand and feedstock activity more reliably across regions, OPERA applies emission-based distribution keys derived from the MIDDEN database (PBL Netherlands Environmental Assessment Agency, n.d.). Table 6: Emission-based spatial distribution of industrial activity (MIDDEN, 2024). summarises the emission-based industry distributions used to disaggregate national industrial demand and feedstock activity to the regional level.

Table 6: Emission-based spatial distribution of industrial activity (MIDDEN, 2024).

Region	Chemical	Refineries	Basic metal non-ferro	Basic metal ferro	Food and beverage	Fertiliser	Industry other
Port of Rotterdam							
Botlek	30%	24%	0%	0%	2%	0%	0%
Europoort	9%	24%	0%	0%	14%	0%	0%
Groot-Rotterdam	0%	0%	0%	0%	0%	0%	0%
Maasvlakte	0%	0%	0%	0%	1%	0%	0%
Pernis	1%	38%	0%	0%	0%	0%	0%
Moerdijk	3%	0%	0%	0%	0%	0%	0%
Rest of NL							
South Holland remaining	7%	0%	5%	0%	15%	0%	7%
Limburg	4%	0%	5%	0%	0%	40%	30%
Mid NL	2%	0%	20%	0%	3%	0%	33%
North Brabant remaining	0%	0%	29%	0%	9%	0%	9%
North Holland	5%	0%	13%	100%	11%	0%	8%
North NL	20%	0%	20%	0%	35%	0%	13%
Zeeland	18%	14%	8%	0%	10%	60%	1%

Taken together, these distribution keys provide a consistent spatial representation of the Dutch energy system within OPERA. They reflect regional variation in industrial activity, energy demand, resource potential, and technology suitability, which is particularly important for assessing transitions with strong spatial constraints, such as decarbonisation pathways for the Port of Rotterdam.

Scenarios

Base Scenario

The Base scenario evaluates how a detailed regionalisation of the Port of Rotterdam industrial cluster affects system outcomes within a Netherlands-wide climate-neutral transition pathway. It assumes a trajectory to net-zero greenhouse gas (GHG) emissions by 2050, with interim reductions of 55% by 2030 and 90% by 2040 relative to the current emissions level. Within the OPERA scenario framework, the Base scenario is used as a proxy for TRANSFORM, a high-ambition sustainability pathway described by Scheepers et al. (2022). TRANSFORM reflects structural shifts in demand and behaviour, including slower growth (or reductions) in material and energy use, higher recycling rates and circularity, and broad efficiency improvements across sectors. On the supply side, the pathway relies on strong scale-up of renewables, particularly offshore wind, alongside high electrification and extensive sector coupling.

In this storyline, biomass availability is constrained to sustainable volumes and directed primarily to applications with limited low-carbon substitutes, while fossil fuels are rapidly phased out. Carbon capture and storage (CCS) is available but is treated as a constrained option, reserved for residual emissions that remain after efficiency measures, electrification, and material substitution have been exhausted. In OPERA, these assumptions are operationalised through tighter sustainability constraints, higher renewable potentials, reduced dependence on fossil-based pathways, and limited CCS availability, yielding a consistent representation of a transformation-oriented transition pathway (Scheepers et al., 2022). Key quantitative inputs for the Base scenario are summarised in Table 7. These parameters mainly act as upper bounds on resource potentials, infrastructure availability, and cross-border trade volumes. Within these bounds, the model endogenously selects the least-cost technology portfolio and energy flows, subject to the GHG reduction constraints.

Table 7: Key assumptions for the Base scenario.

Assumption	Unit	2030	2040	2050
GHG emission reduction	%	55	90	100
Offshore wind potential	GW	16	45	70
Onshore wind potential	GW	8	10	12
Solar PV potential	GW	43	84	132
Nuclear potential	GW	0.5	3.5	6
Biomass potential	PJ	118	407	697
Domestic CCS potential	$MtCO_2/yr$	13	15	15
Electricity imports	TWh/yr	39	37	37
Electricity exports	TWh/yr	24	39	49

Alternative Scenarios

To examine how the Port of Rotterdam's system role may evolve under different strategic and policy settings, we evaluated a set of alternative scenarios for 2040 and 2050. The scenario set is built around uncertainties that are especially consequential for port-industrial clusters: (i) the pace and configuration of nuclear capacity deployment, (ii) the scale and reliance on imported renewable fuels, and (iii) the potential for ports, acting as transition nodes, to face tighter, regionally differentiated climate targets (Damman et al., 2025).

The alternative scenarios are:

- *RESfuel_Imp*: Imports of renewable fuels are permitted, covering both biofuels (e.g., bioethanol, biodiesel, biokerosene) and synthetic fuels (e.g., synthetic methanol, synthetic kerosene). Total import volumes are capped at 70 PJ (2040) and 110 PJ (2050) for biofuels and capped at the same levels for synthetic fuels. The model determines the optimal split across specific fuel types endogenously. Exports of renewable fuels are not allowed, to keep the focus on domestic final demand rather than transit or re-export functions.
- *NoNuc*: Nuclear generation is allowed at the national level up to 6 GW, but no nuclear capacity is permitted within the Port of Rotterdam region.
- *SMR*: Conventional large-scale nuclear is excluded, while small modular reactors (SMRs) are allowed within the Port of Rotterdam up to a total capacity of 0.5 GW. Siting and dispatch are determined endogenously by the model.
- *NetZero_PoR*: Beyond the national net-zero GHG constraint, the Port of Rotterdam region (including Groot-Rotterdam) must also achieve net-zero emissions, implying stricter regional constraints on energy production, conversion activities, and residual emissions.

All alternative scenarios are run under both spatial configurations, with and without the detailed regionalisation of the Port of Rotterdam. This design supports a structured comparison of (i) how added spatial detail changes system outcomes under strategic uncertainty, and (ii) how port-specific constraints propagate into the wider national energy system. Results from OPERA regarding industrial electricity demand in the port region will be used by the EUR Energy Model in section 3.6. Furthermore, H_2 demand for all modelled regions in the Netherlands will be used by the H2 Distribution Model in section 3.7. These links are necessary to ensuring consistency between national projections for the electrification of industrial processes in the port and the H2 demand.

3.5 EWI Global Power to X Cost Tool

The EWI Global PtX Cost Tool V2.1 provides detailed scenarios for the global supply side of green hydrogen and hydrogen derivatives from wind and solar energy. The scenario outputs of the WITCH IAM can be used as base trends for the hydrogen demand. The tool enables the analysis of production costs and production potential from 116 origin countries, as well as the transportation costs from these origin countries to 22 destination countries. The tool covers hydrogen as well as the hydrogen derivatives ammonia, methane, methanol and fischer-tropsch-fuels, and LOHC. It is an open-source tool and available for download at the EWI website[1]. Key features of the model are described in the table below.

Table 8: EWI Model summary

Aspect	Description
Space	Global (116 origin countries and 22 destination countries)
Time Step	Calculation: Hourly resolution, results: monthly resolution
Era	2025, 2030, 2035, 2040, 2045, 2050
Carriers	Hydrogen, Methane, Methanol, Fischer-Tropsch Fuel, Ammonia, LOHC (all hydrogen based and based on PV, onshore wind, and offshore wind, and CO2 Direct Air Capuring for Methane, Methanol, and Fischer-Tropsch fuel)
Objective	Calculating production and transportation costs
Method	Optimization model

The supply cost estimation follows a three-step approach, as shown in Figure 16: Methodological approach of the EWI Global PtX Cost Tool V2.1 In the first step, we collect all input parameters in a meta-analysis. In the second step, we estimate the production costs in the origin countries using a linear optimization program modelling integrated production plants with dedicated renewable energy sources (RES). In the third step, we calculate the transport costs for an assumed default utilization of the transport infrastructure. All costs are expressed in USD 2024. Where necessary, we converted cost data from other currencies and years to USD 2024 using historical exchange rates and inflation. Caloric energy units refer to the lower heating value.

[1] https://www.ewi.uni-koeln.de/en/publications/ewi-global-ptx-cost-tool-v2-1/

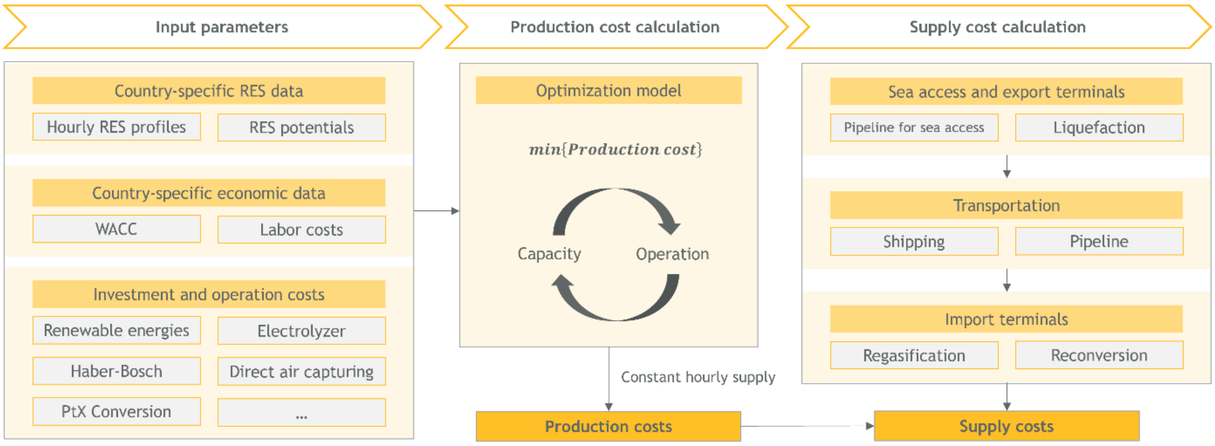

Figure 16: Methodological approach of the EWI Global PtX Cost Tool V2.1

In the following, the most relevant input parameters are presented, the production cost calculation, and the supply cost calculation. The quantitative values of all parameters including their sources are provided in the tool itself. Further information on the methodology are provided in the documentation of the tool which is available at the download section of the tool.

Input parameters

A meta-analysis for the techno-economic properties of all technologies involved in green hydrogen production and conversion to derivatives was concluded. Based on this analysis, a baseline and an optimistic scenario to assess the future development of these properties from 2025 to 2050 was designed, but any scenario (like those from WITCH IAM) can be used as input. In both scenarios, the values for 2025 represent the current techno-economic properties. From the year 2030 onwards, we calculate cost degressions based on learning and economies of scale effects, when applicable. Learning rates are assumed for electrolyzer stacks, renewable energy sources, and CO2 direct air capturing plants. For the baseline scenario, we choose learning rates that represent the average found in other projections from the literature. For the optimistic scenario, we choose higher learning rates that resemble a more optimistic market acceleration. Economies of scale effects are assumed for electrolyzer balance of plant components as well as all conversion plants and are calculated based on the 70% rule, meaning that investment costs increase by 70\% when the reference plant size is doubled (Cooper, 2007). In the baseline scenario, reference plant sizes are assumed to increase from 100 MW in the year 2025 to 250 MW in the year 2050. In the optimistic scenario, reference plant sizes increase from 100 MW in the year 2025 to 1,000 MW in the year 2050.

Country-specific Weighted Average Cost of Capital (WACC) and labour costs are used for the production and transport cost calculation. The real WACC is based on the nominal WACC and the expected inflation in the US. The nominal WACC comprises a base interest rate, a country risk premium as shown by Damodaran (2025), an equity risk premium, and a technology risk premium. As a result, we calculate with a real WACC of 7.2% in AAA-rated countries that increases to up to 26.6% in C-rated countries. Costs for international pipeline infrastructure and vessels are calculated with a uniform WACC of 10%. Investment costs and fixed operations and maintenance (fom) costs are adjusted through country-specific labour costs. In the first step, we define investment and form costs for the OECD labour costs average. Then, we define a labour costs share and adjust investment and fom costs based on country-specific and OECD average labour costs. We define a labour cost share of 40 %

for conversion plants based on Peters et al. (1991). For electrolyzers and CO2 DAC plants, we define a labour cost share of 20 % in the deployment country, as research and development might rather take place in developed countries near OECD average labour costs. For RES, we vary investment and fom costs in ten world regions based on labour costs and manufacturing capabilities from DNV (2024). Country-specific labour costs from the year 2024 are taken from ILO (2025).

Renewable energy sources for powering the electrolyzer are classified in an approach adopted from Brändle et al. (2021). PV and wind onshore potentials are classified by their capacity factor, which equals average capacity divided by nominal capacity. Wind offshore potentials are classified by the water depth, as the depth drives the investment costs. We exclude potentials below certain capacity factor thresholds or, in the case of wind offshore, above a water depth of 60 m because production from these potentials would hardly be economical. Country-level PV capacity factors and potentials (installable capacity) are taken from Pietzcker et al. (2014). Remote potentials with a distance of more than 50 km to the next settlement are excluded. Capacity factors and potentials for wind onshore are taken from Bosch et al. (2017). Capacity factors and potentials by water depth for wind offshore are taken from Bosch et al. (2018). Hourly profiles for each country are selected and each RES class from Renewables Ninja based on locations from Global-Wind-Atlas (2024) and Global-Solar-Atlas (2024).

For renewable energy investment costs, two scenario projections are based on cost data from recent real projects and cost projections found in the literature. A baseline was constructed and a optimistic scenario projection starting at the same fixed point in 2025, which represents current investment costs and ending at two different fixed points in 2050 based on projections from literature. For renewable energy technologies, three fixed points for each technology are selected to determine the trajectory of investment costs. The first fixed point is set in 2025, representing the current state of investment costs, and serves as the starting point for both the baseline and the optimistic scenario. Two additional fixed points are defined for 2050, one for each scenario, based on literature projections of investment costs. These fixed points are determined through two independent analyses of existing techno-economic studies. The 2050 baseline fixed point corresponds to the mean of the available literature data, whereas the 2050 optimistic fixed point corresponds to the lower quartile (25%) of the literature distribution.

Hydrogen production by water electrolysis is considered. Among existing water electrolysis types, focus is on alkaline (AEL) and proton-exchange-membrane electrolyzers (PEMEL) as they are mature technologies. Both electrolyzer types are projected to have similar investment costs. For the estimation of the electrolyzer investment cost development, we define three fixed points following the same approach as for RES. The first fixed point is set in 2025 and represents current investment costs based on the data provided by Observatory (2024). These data represent investment costs for a project of 100 MWel total size in an advanced project stage, derived from an annual industry survey. Investment costs are disaggregated into four categories: stack, balance of plant (BoP), other utilities, and other CAPEX. For the cost development until, we conduct a meta-analysis and consider economies of scale effects and learning rates. For most PtX conversion processes, we derive cost and efficiency data analogous to Moritz et al. (2023).

Production cost calculation

An optimization model was used to calculate the production costs of each commodity for each RES class in each origin country. The model determines the optimal capacities and operation of an integrated production plant using a dedicated RES plant to minimize production costs to cover an inelastic demand. The model flow sheet for the production cost calculation is provided in Figure 17.

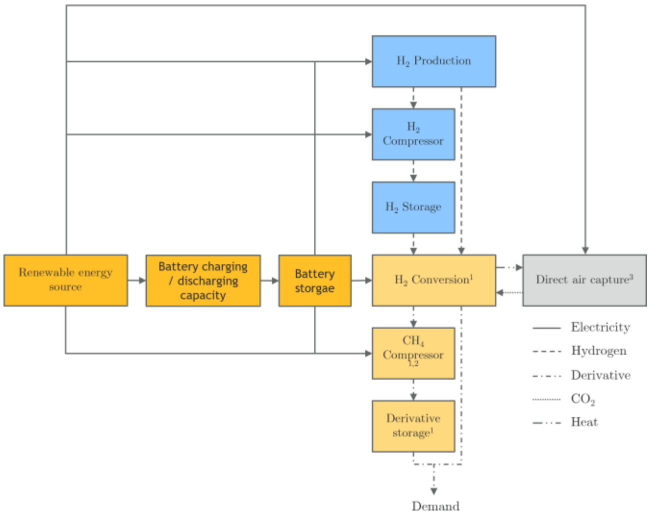

Figure 17: Model flow sheet for production cost calculation

Transport cost calculation

Transportation costs are calculated ex post to the production costs, depending on the supply route. Transportation costs through pipeline and shipping are calculated for all commodities, as shown in **Fout! Verwijzingsbron niet gevonden.**. For calculating the distance between two countries, the capital of the origin country is used as the starting point and the capital of the destination country as the endpoint. Pipeline transport between countries is only an option if a natural gas pipeline infrastructure currently exists and the distance is assumed according to the current pipeline route. Pipeline transportation costs are calculated for newly constructed pipelines and, in the case of hydrogen, for retrofitted natural gas pipelines. Pipeline transportation costs are also calculated between the capital and the port of origin country, and the port and capital of the destination country for maritime transport routes. For hydrogen, we calculate shipping costs in the form of liquefied hydrogen (LH2), ammonia, and liquid organic hydrogen carriers (LOHC). In the case of ammonia and LOHC, the conversion step from hydrogen to ammonia or LOHC already takes place in the integrated optimization model. In the case of LH2 and methane, we calculate liquefaction costs at the port. Shipping costs are calculated based on a total ownership approach of the vessels for the commodities. All vessels are powered with green methanol. We assume shuttle operation and include waiting time, berthing time, port fees, and refuelling costs in the cost calculation. In the port of the destination country, we calculate the regasification costs for LH2 and methane, or the reconversion costs for dehydrogenation for LOHC and ammonia cracking for ammonia. For both these processes, hydrogen is used to cover the heat demand. Furthermore, we calculate all transport costs for a greenfield and a brownfield scenario where only operation and maintenance costs for pipeline and terminal infrastructure are considered.

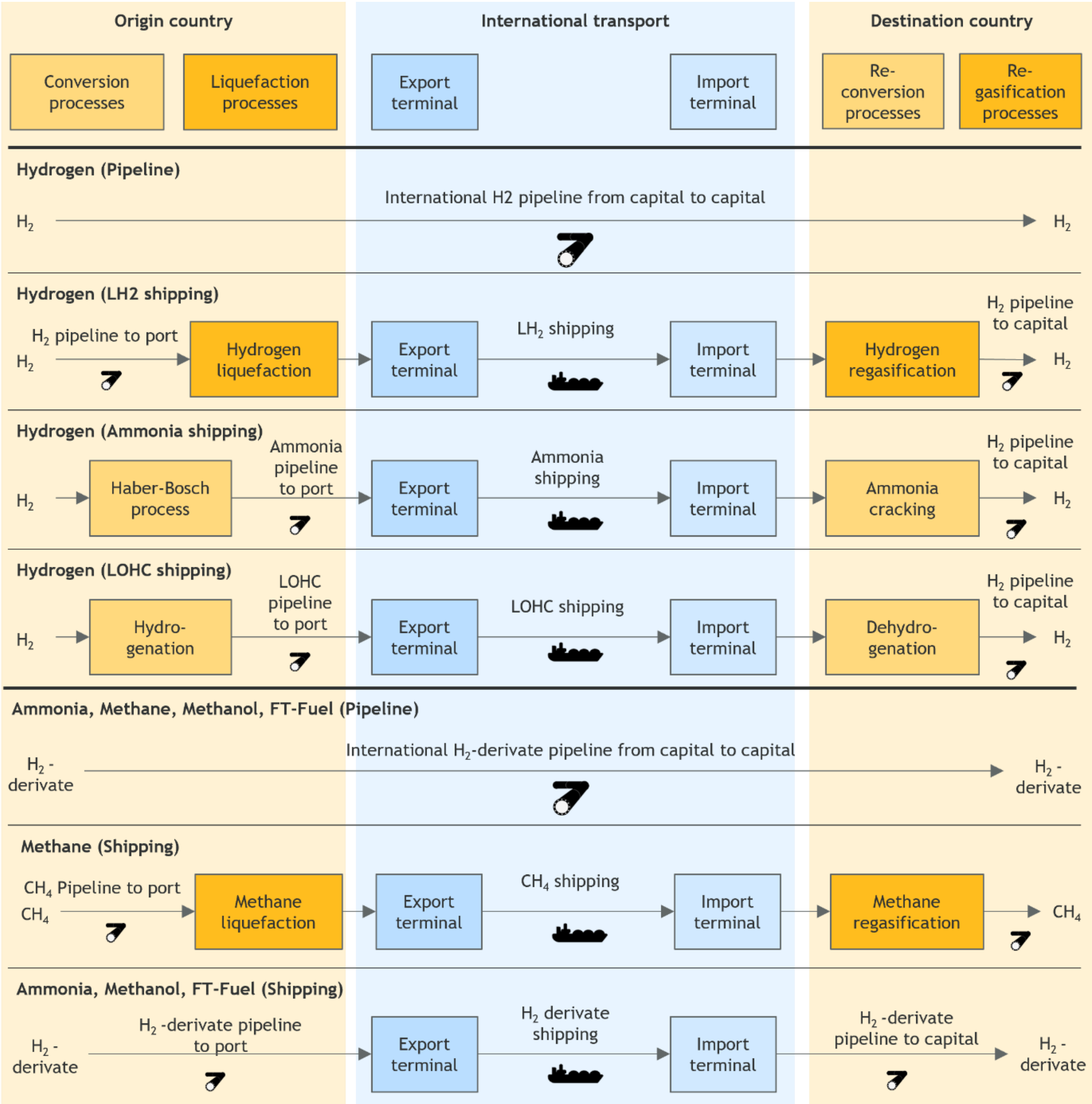

Figure 18: Transportation routes for transport cost calculation

3.6 EUR Energy Model

As a majority of the demand sectors in the port move toward electrification—including industrial processes and the shift toward electric trucks—the stress on the local distribution grid increases substantially. Although the overall direction of electrification is clear, the magnitude and temporal patterns of future electricity demand and supply remain highly uncertain. This uncertainty is further intensified by the variability of renewable electricity generation, such as wind power produced within the Port of Rotterdam.

These developments collectively heighten pressure on the existing grid infrastructure, making it increasingly difficult to ensure that supply and demand remain balanced under all operating conditions. One of the most pressing challenges arising from this situation is grid congestion, which occurs when electricity flows exceed the technical capacity of grid assets required to maintain supply-demand balance (IRENA, 2022). As both the variability and the total volume of load and generation grow, congestion becomes a systemic risk for secure electricity delivery. The consequences are particularly severe in power systems governed by strict reliability standards, where acceptable outage frequencies may be fewer than one day over a ten-year horizon (Electric Power Research Institute, 2022). Persistent or recurring congestion not only raises the likelihood of supply interruptions but also delays, limits, or prevents new grid connections for businesses, creating significant economic impacts (IEA, 2024).

Table 9: EUR model summary

Aspect	Description
Space	Local Microgrid (e.g. Port of Rotterdam)
Time Step	Hourly
Era	One year (Can be any year up to 2050 as a scenario)
Carriers	Electricity
Objective	Lowest cost and CO2 emissions energy system with threshold for Loss of Load Probability (LOLP)
Method	Stochastic Programming / Robust Optimization where we incorporate uncertainty in demand and renewable energy output

In this context, our objective is to understand how ongoing electrification and renewable integration affect the need for a resilient distribution grid, and how uncertainties in demand and supply can be systematically incorporated into decision-making. Specifically, we focus on supporting strategic, long-term planning aimed at minimizing costs while accounting for congestion resulting from increased electrification and variability in demand and supply. We examine these questions from two complementary and interdependent angles: i) investment decisions, including capacity upgrades and battery installations, which ensure the grid can accommodate future load growth efficiently, and ii) operational decisions required to maintain system balance while satisfying stringent reliability requirements. By integrating these perspectives, our approach provides a framework for making informed, cost-effective decisions that proactively address the challenges posed by the evolving energy landscape.

Crucially, these two perspectives influence one another. Operational feasibility under uncertain conditions determines the scale and type of investments required, while the investment choices, in turn, shape the operational flexibility available to the grid operator. Therefore, we integrate both types of decisions in a single optimization framework. This framework consists of two interconnected layers: in the first layer, we determine investment decisions for grid line capacity and battery sizing at each node; in the second layer, we solve a multi-period operational model—referred to as (RGOP)—that governs operational decisions $\boldsymbol{y}$ such as battery charging and discharging and import/export from the upstream grid where we can use flexibility from batteries to shift consumption and production over time.

The objective of the model is to minimize total investment and operational costs. Let $\theta \in \Theta$ be distinct independent scenarios, such as days of the week and seasons and,

$$\mathbb{E}[V(x)] = \sum_{\theta \in \Theta} v_\theta V_\theta(x)$$

is approximated as a weighted sum of $V_\theta(x)$, the operating costs of scenario θ with the distribution of the uncertainties defined according to the scenario. The resulting model is the Grid Investment Problem (GIP):

$$\min \sum_{m \in M} \kappa_m^{ESS} x_m^{ESS} + \kappa_m^G x_m^G + \sum_{e \in E} \kappa_e^{inter} x_e^{inter} + \sum_{\theta \in \Theta} v_\theta V_\theta(x)$$

$$\text{s.t. } x_m^{ESS} \le \bar{\kappa}^{ESS}$$

$$x_m^G \le \bar{\kappa}^G$$

$$x_e^{inter} \le \bar{\kappa}^{inter}$$

where κ_m^{ESS}, κ_m^G, and κ_e^{inter} are the levelized investment costs per unit size of the battery, external grid, and internal grid investments respectively, accounting for the different lifetimes of battery and grid power line investments. The operational problem is given as:

$$V(x) \coloneqq min_y \, sup_{\mathbb{P} \in F} \, \mathbb{E}[\boldsymbol{c}^T \boldsymbol{y}]$$

$$s.t. \; \boldsymbol{y} \in Y(\boldsymbol{x}),$$

where y represents the operational decisions, $\boldsymbol{c}$ their corresponding costs, and

$Y(\boldsymbol{x})$ the feasible set defined by constraints such as battery charging and discharging limits, state-of-charge bounds, grid line flow limits, and power balance constraints. The uncertainty vector q captures fluctuations in wind generation and in industrial and electric truck demand. All realizations of q lie within the uncertainty set F, and the model identifies operational decisions that are optimal under the worst-case realization in that set. For more details on the model formulation and how the model is solved, we refer to the academic paper for this model (Punt et Al., 2024).

In our analysis, we use a simplified network, consisting of two nodes, a production node with wind generation and a consumption node representing a small area in the port with electricity demand from industry and electric truck charging. This simplified structure allows us to isolate the effects of local electrification and renewable variability while preserving the fundamental interactions between generation, consumption, storage, and the wider grid.

Wind generation in the port is modelled using their installed capacity of approximately 330 MW (Port of Rotterdam, n.d.), compared to the maximum capacity in the Netherlands of 6,000 MW. The temporal profile of generation is derived from historical data via the Energieopwek.nl dashboard (Energie Opwek Nederland, 2025) and accordingly scaled to align with the port area. The production node is connected internally to the consumption node and externally to the upstream grid, and batteries can be installed at this node to store excess wind energy that cannot be immediately consumed, enhancing operational flexibility and reducing curtailment.

Electricity demand at the consumption node combines industrial demand and electric truck charging demand. **Industrial demand is aligned with the TNO Transform scenario** (Elberry et al, 2025, TNO, 2024), ensuring consistency with national projections for the electrification of industrial processes in the port. The temporal resolution is hourly, and scenarios capture daily and seasonal variations. Electric truck charging demand is represented in an aggregate demand profile and derived from the ElaadNL charging simulator (ElaadNL, n.d.) and port infrastructure information (Port of Rotterdam, n.d.). The port has eight charging bays distributed across five charging points, including three terminals with two connectors each and two fast chargers with one connector each. On average, each charging point provides approximately 360 kW, and trucks are assumed to charge when parked at these points. Importantly, we do not explicitly specify the number of trucks or projections thereof. Instead, the aggregate charging demand is captured indirectly through the available charging capacity. By assuming that the installed capacity is sufficient to meet the required charging needs, the simulator produces charging profiles that reflect feasible utilisation patterns under the given infrastructure. By providing the charging capacity and type of charging point to the simulator, we can generate different charging profile scenarios that can be incorporated into our data and uncertainty set.

To capture projected growth and its associated uncertainty in both supply and demand, we supplement the TNO Transform scenario with projected growth factors from the Netbeheer Nederland Outlook 2030-2050 scenarios (Netbeheer Nederland, 2023). These scenarios provide projected increases in wind generation, industrial demand, and electric transport across the Netherlands. Because the uncertainty set is constructed directly from the data, including its moments and bounds, applying these growth factors multiplicatively to the data ensures that the resulting uncertainty set is adjusted consistently.

3.7 EDP – H2 Distribution Model

This model is a techno-economic simulation framework that evaluates all feasible carrier-transport scenarios for hydrogen distribution from a port to all H2 Hubs (single offtaker or distribution centre). For each carrier-transport combination (e.g., GH2/LH2 with truck, barge, or pipeline where applicable), it computes required infrastructure and operating needs, such as number of vehicles, trips, storage capacity, (re)conversion units (e.g. compression), or pipeline sizing and routing, and estimates the corresponding transportation cost.

A more detailed description of the formulation, assumptions, and results for long-term scenarios can be found in D.3.5. To assess long-term scenarios, the model relies on exogenous inputs produced by external models, such as H_2 demand projections for different regions in the Netherlands from OPERA (influenced by WITCH model), as well as carrier-specific costs from the PtX model, which vary depending on whether the H_2 carrier is imported by sea or produced locally, as shown in Table 10.

Table 10: Hydrogen model summary

Aspect	Description
Space	Port to H2 Offtakers
Time Step	Hourly H2 demand profiles utilized to estimate transportation costs given as unique value
Era	Strategic planning for future hydrogen deployment (e.g. now until 2050 scenario), evaluated over a representative operating year with annualized costs.

Carriers	GH2, LH2 (subject to modality feasibility, e.g., pipeline only with GH2).
Objective	Evaluate and compare all feasible carrier-transport scenarios for all offtakers, identifying their cost and infrastructure implications for hydrogen delivery
Method	Deterministic economic scenarios, where each carrier-transport combination is simulated independently; transport requirements, equipment sizing, and total annualized costs are calculated and compared across scenarios.

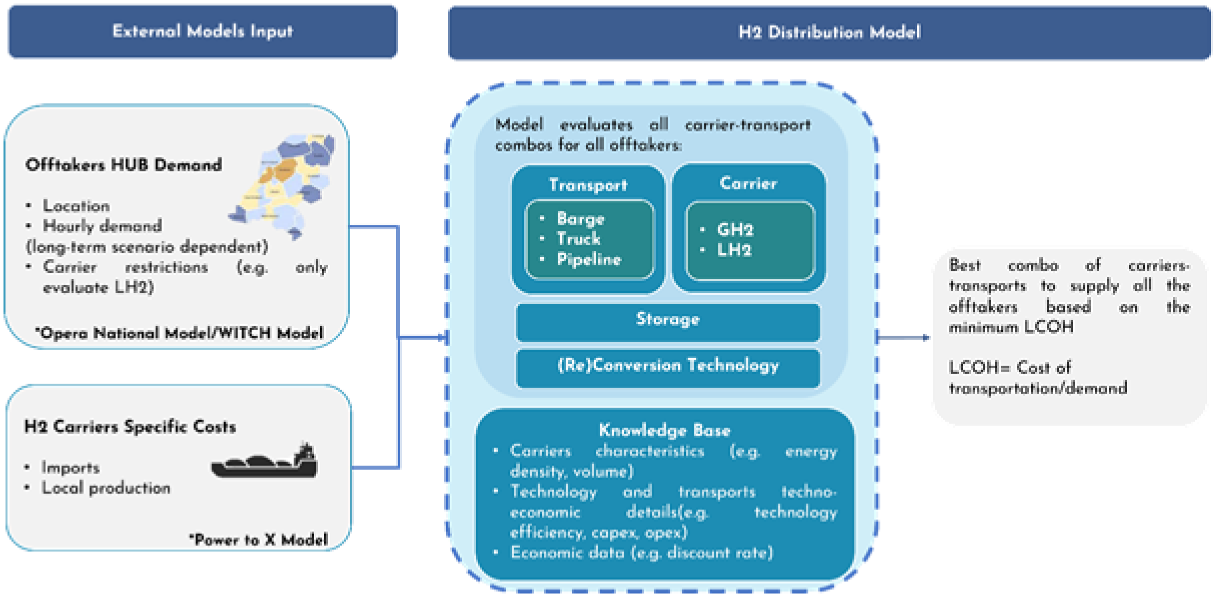

Figure 19: H2 distribution model overview and links to external models

3.8 EDP Recharging Assessment Model

This model is a simulation rule-based framework that evaluates electric-truck energy demand across inbound/outbound truck routes associated to ports. For each simulated trip, the model tracks battery state-of-charge dynamics, route progress, charging needs, and charging opportunity windows, treating each trip independently before aggregating system-level outcomes. Based on these trip-level results, it identifies where and when charging is likely to occur and its magnitude, generating heat maps of charging activity.

A more detailed description of the formulation, assumptions, and results for long-term scenarios can be found in D.3.3. To assess long-term scenarios, the model relies on exogenous inputs produced by the WITCH Model, like the ratio of electrified truck fleet projections and freight growth assumptions, and can also be influenced by the charging infrastructure rollout which impact on the magnitude and distribution of demand, as shown in Table 11.

Table 11: Truck demand model summary

Aspect	Description
Space	Port and Hinterland truck routes
Time Step	15min time-steps
Era	One or more representative weeks (can be adapted to different long-term scenarios)
Carriers	Electricity (with potential extension to other carriers such as H2 refuelling)
Objective	Creation of heat maps showing where electric trucks will recharge their batteries and creation of demand profile for electric truck charging in the port area
Method	Simulation-based approach in which each truck trip is evaluated independently

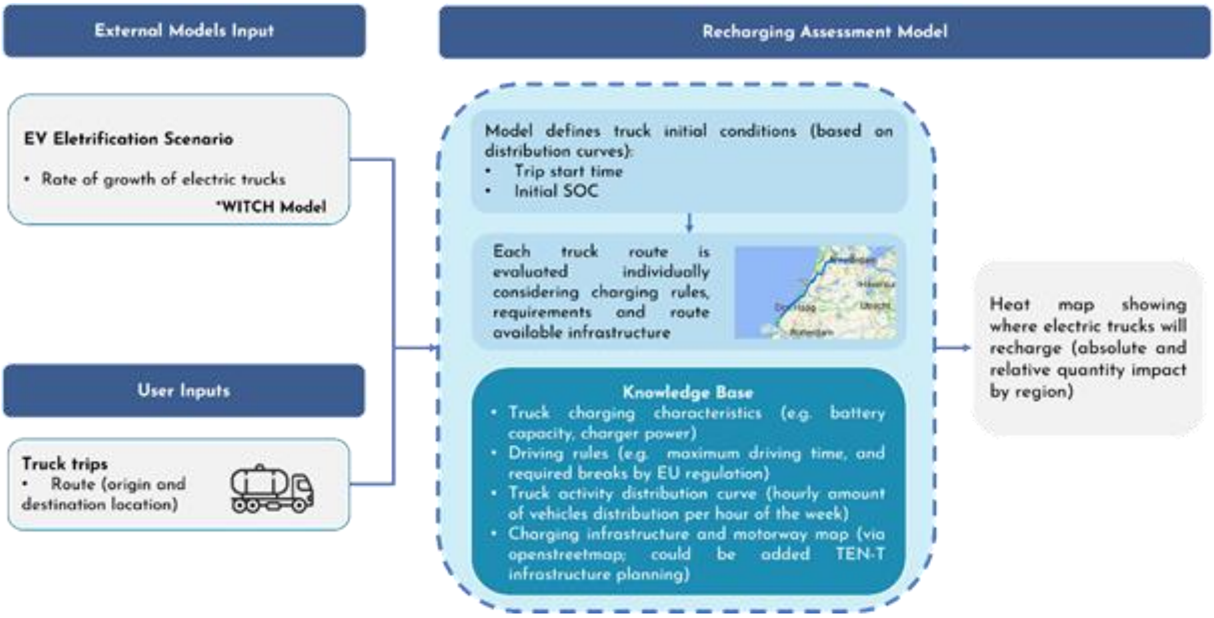

Figure 20: Recharging Assessment model overview and links to external models

4. Model Results

This chapter will demonstrate and discuss key results from scenarios run in each model, not going into the details of each demonstrator or MAGPIE solution (that will be done as indicated in the WP7-9). The focus here is on the supply demand predictions up to 2050 (using 2030,2040 and 2050 as key years where models have a smaller time scale).

4.1 WITCH IAM with TUD Extension

Shipping activity demand

Figure 21 shows that seaborne shipping demand increases over time in all scenarios, but the growth is consistently stronger in the baseline-based pathways than in the 1.5°C-based pathways. This difference is expected. In the mitigated scenarios, stricter climate policy raises abatement costs and fuel prices, reduces fossil-fuel trade, and slightly lowers overall economic growth, which together dampen trade volumes and therefore shipping activity. The reduction is most visible for fossil-energy-related cargoes, especially oil and oil products, while non-energy cargoes remain more resilient. In the baseline-based case, global demand continues to rise strongly throughout the century, whereas in the 1.5°C-based case growth is visibly moderated, consistent with earlier findings that stricter carbon policies reduce seaborne trade mainly through lower fossil-fuel trade and higher transport costs.

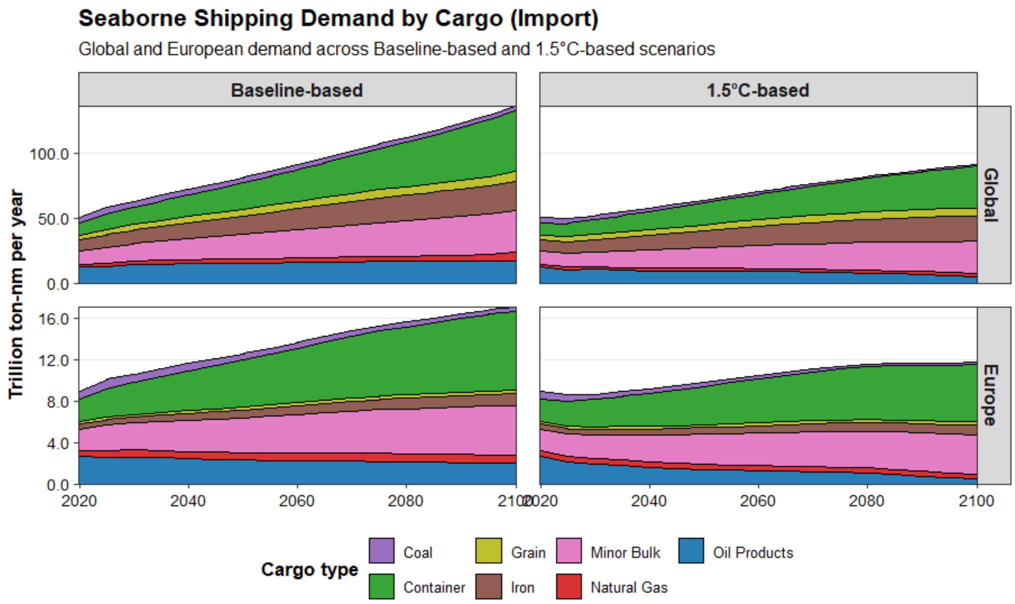

Figure 21: Shipping demand scenarios by cargo

The cargo composition also changes over time. Oil products and natural gas decline more strongly under mitigation, reflecting the direct effect of climate policy on fossil-fuel production and consumption patterns, while coal shows a structural downward trend across scenarios. By contrast, containerized cargo, minor bulk, grains, and iron ore generally continue to increase, although with a lower slope in the 1.5°C-based pathways. This is in line with the broader result that iron ore and grains are less sensitive to climate policy and remain mainly driven by economic and demographic growth, whereas containerized and minor bulk cargoes keep expanding but more slowly under stringent mitigation.

For Western Europe, the contrast between scenarios is particularly clear. In the baseline-based pathway, total seaborne import demand approximately doubles by 2100, while in the 1.5°C-based pathway it rises by only around half relative to 2020. Much of this divergence comes from the sharp reduction in oil and oil-product imports under climate mitigation, while containerized cargo and non-energy bulks continue to grow and gradually take a larger share of total demand. In other words, mitigation does not remove growth in shipping demand, but it shifts the composition away from fossil-energy cargoes and toward more resilient trade categories. This pattern is fully consistent with the paper's broader conclusion that baseline-based pathways show higher endogenous activity levels because higher economic growth and lower fuel prices sustain larger shipping demand, whereas 1.5°C pathways reduce demand mainly by curbing fossil-fuel trade.

Shipping Fuel mix

Figure 22 summarises the global shipping fuel transition across all scenarios and is best read panel by panel. In panel (a), the annual fuel-mix trajectories show that the BAU case remains dominated by oil-based fuels throughout the century, with only a slow and limited shift toward LNG. Under the 1.5deg pathway, the transition is much stronger but still gradual: oil declines after mid-century and ammonia expands steadily as hydrogen and ammonia supply chains scale up and become more cost-competitive. The 1.5deg-IMO case moves faster, reaching an almost fully ammonia-based system around mid-century, with biofuels covering the residual share. By contrast, 1.5deg-NA, where ammonia is excluded, produces a fragmented transition: oil remains dominant for much longer, methanol and biofuels expand as second-best options, and small amounts of direct hydrogen appear in short-haul segments. This delay reflects the loss of the most scalable zero-carbon marine fuel. The two MEPC-based cases also shift the sector earlier than the corresponding economy-wide pathways, but they do so differently: in 1.5deg-MEPC, ammonia rapidly becomes dominant and oil is displaced very early, while in BAU-MEPC the transition is more mixed, with a substantial early and persistent role for biofuels, a continued but declining contribution from oil and LNG, and a later expansion of ammonia. This is consistent with the broader result that shipping-specific policy accelerates the transition in the sector more directly than global mitigation policy alone. Across all ambitious scenarios in which ammonia is allowed, ammonia becomes dominant because it is scalable, does not require carbon inputs, and remains cost-competitive once clean hydrogen and Haber–Bosch capacity expand.

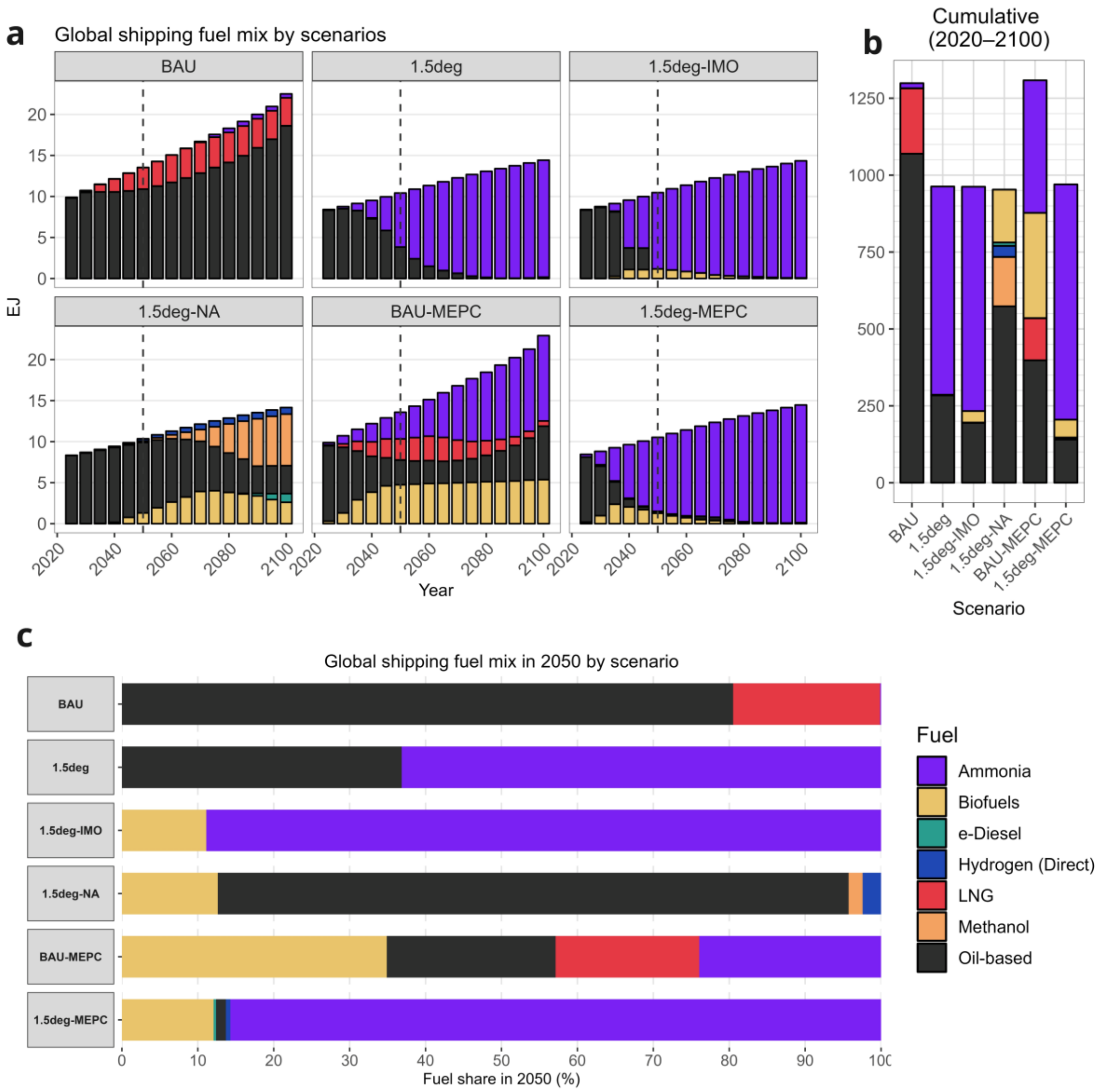

Figure 22: Aggregated Shipping Fuel use per Scenario

Panel (b) shows cumulative fuel use over 2020–2100 and confirms the same ranking from another angle. Baseline-based pathways have the largest cumulative energy use because shipping demand is higher under stronger economic growth and lower fuel prices. A substantial part of this comes from larger trade in oil and petroleum products. In contrast, the 1.5deg and 1.5deg-IMO scenarios cut cumulative fossil-fuel use sharply, while ammonia provides the majority of cumulative energy in ambitious pathways. Biofuels play a secondary but visible role, especially in BAU-MEPC, where they account for a large share of cumulative fuel use and act as the main transition fuel before ammonia becomes more important.

Panel (c) then makes the mid-century structure clearer. By 2050, most decarbonisation pathways are already ammonia-led, complemented by biofuels and only small shares of e-diesel and direct hydrogen. The clearest exception is 1.5deg-NA, where oil still dominates in 2050 and even exceeds the oil share in BAU at that point, because other sectors compete strongly for low-carbon fuels while shipping loses access to ammonia. BAU-MEPC is another important exception: by 2050 it is not yet ammonia-led, but instead shows a more balanced mix in which biofuels are the largest low-carbon component, oil still retains a substantial share, LNG remains relevant, and ammonia has expanded but not yet taken over. Together, the three panels show that the transition is shaped less by carbon-pricing stringency alone than by the availability and scalability of genuinely zero-carbon marine fuels.

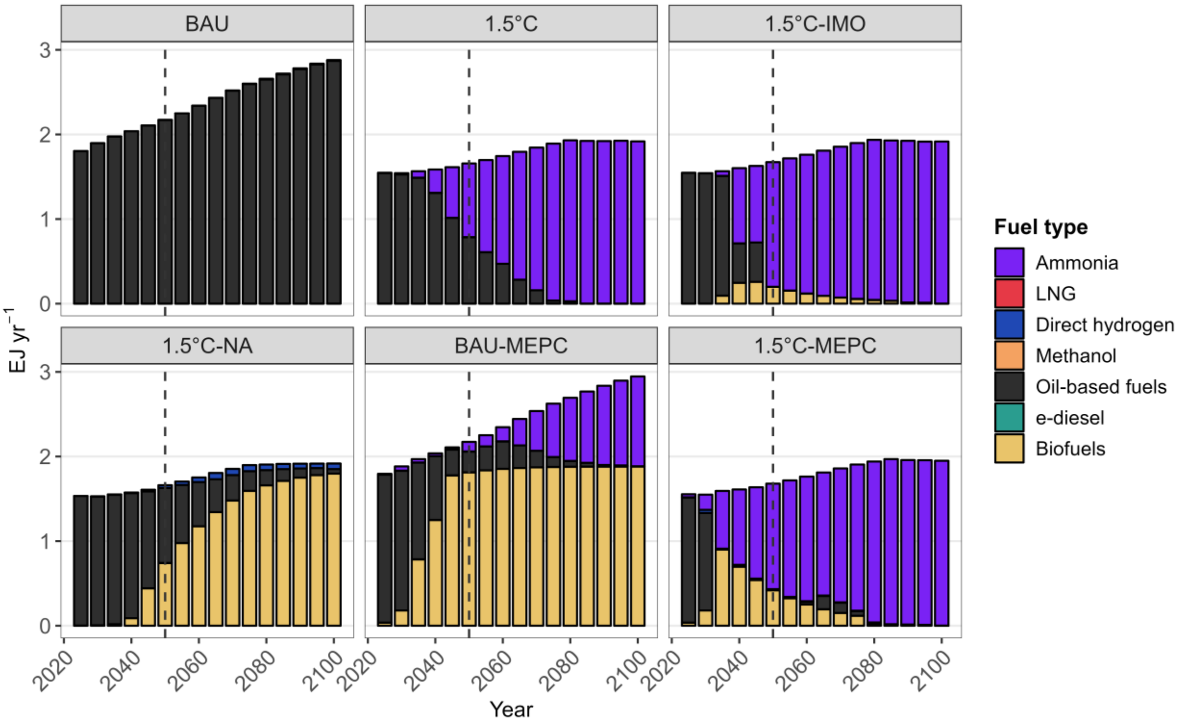

Figure 23: European Shipping Fuel Use

Figure 23 shows the same set of scenarios for Europe, but with some important regional differences. The overall pattern remains the same: BAU stays oil-based, 1.5deg and 1.5deg-IMO become ammonia-led, and 1.5deg-MEPC reaches an almost complete transition by the end of the century. However, Europe exhibits an even stronger role for biofuels than in the global results, especially in BAU-MEPC and in the ammonia-ban case, 1.5deg-NA. In both scenarios, biofuels become the main transition fuel and remain important in the long term, while ammonia either expands more gradually or is excluded altogether. In BAU-MEPC, biofuels dominate early and continue to provide a large share of the fuel mix throughout the century, with ammonia rising steadily in parallel. In 1.5deg-MEPC, by contrast, biofuels play a more clearly transitional role: they rise early, help reduce oil use quickly, and are then progressively overtaken by ammonia as zero-carbon hydrogen and ammonia supply chains mature. This is exactly the pattern expected when shipping-specific policy forces early action before the lowest-cost long-run fuel has fully scaled.

The European results also show that LNG is nearly absent in BAU. The reason is cost-effectiveness in the model: LNG offers only limited decarbonisation benefits, still depends on fossil gas, and does not become attractive enough to displace oil at scale when there is no strong climate or shipping-specific policy forcing. This is consistent with the global result that LNG remains limited mainly to baseline conditions and never becomes a dominant transition fuel. Likewise, direct hydrogen appears only in very small quantities, mainly in the 1.5deg-NA case, because it is mainly suited to short-haul applications and cannot easily scale to the full long-distance marine market. When ammonia is not available, hydrogen therefore enters only at the margin, while biofuels take on the main compensating role and methanol remains negligible. Overall, the European figure reinforces the global conclusion but shows more clearly that the transition can follow different regional sequences: biofuels can act as a strong bridge fuel where available, but long-run deep decarbonisation remains overwhelmingly ammonia-led whenever ammonia is allowed. Without ammonia, the transition slows down sharply and remains much more dependent on biofuels.

Shipping CO2 Emission

Figure 24 shows strong divergence in shipping emissions across scenarios. In panel **(a)**, **BAU** emissions rise continuously to above 2 $GtCO_2\ yr^{-1}$ by 2100, while **1.5deg** reduces emissions more gradually and reaches near-zero only late in the century. **1.5deg-IMO** and **1.5deg-MEPC** decarbonise much faster, reaching near-zero emissions around or before mid-century. By contrast, **1.5deg-NA** declines much more slowly, confirming that excluding ammonia significantly delays shipping decarbonisation. **BAU-MEPC** now shows a clearly different pattern: emissions initially decline, but then rise again after mid-century and remain far above zero by 2100. This reflects the weaker decarbonisation pressure of a shipping-specific policy applied in an otherwise baseline world, where fossil-based demand remains higher and low-carbon fuel switching is not sufficient to eliminate emissions. Relative to the AR6 pathways, BAU lies at the high end, while the mitigation cases decline more rapidly because the model includes stronger sector-specific fuel switching and policy effects.

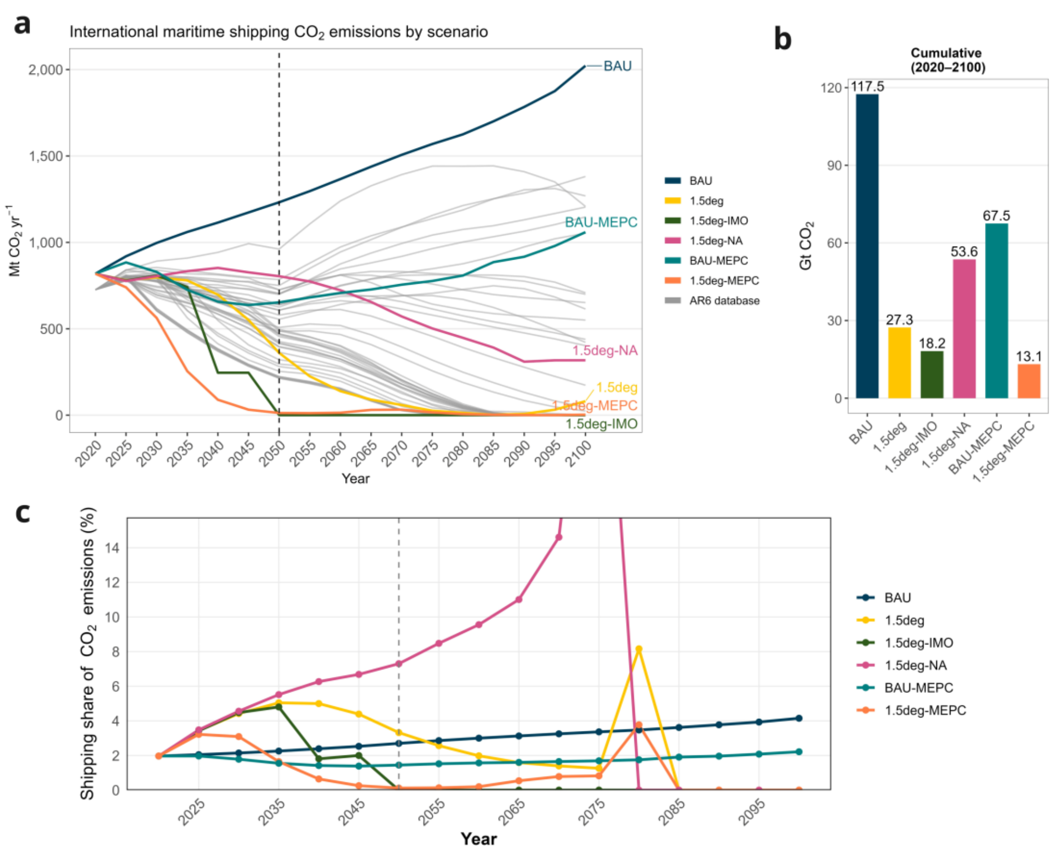

Figure 24: GHG emission panel

Panel **(b)** shows the cumulative effect. Over 2020–2100, emissions fall from about **117 $GtCO_2$** in **BAU** to **27 $GtCO_2$** in **1.5deg** and **18 $GtCO_2$** in **1.5deg-IMO**. The ammonia-ban case remains much higher at about **54 $GtCO_2$**, while **1.5deg-MEPC** achieves the lowest total, around **13 $GtCO_2$**. **BAU-MEPC**, however, is now much higher, at around **68 $GtCO_2$**, showing that shipping-specific policy alone can reduce emissions substantially relative to BAU, but not nearly as effectively as when it is combined with wider economy-wide climate mitigation.

Panel **(c)** places shipping in the wider system. In **BAU**, shipping's share of global CO_2 emissions rises over time. In **1.5deg** and **1.5deg-IMO**, the share increases temporarily and then declines as shipping decarbonises. In **1.5deg-NA**, the share rises much more strongly because the rest of the economy decarbonises faster than shipping. In **1.5deg-MEPC**, shipping's share falls quickly toward zero. **BAU-MEPC**, by contrast, keeps shipping's share relatively low and stable, but does not bring it close to zero. Overall, the figure shows that global climate ambition alone is not enough for rapid shipping decarbonisation; sector-specific policy and ammonia availability are decisive, but sector-specific policy is far more effective when combined with economy-wide mitigation.

System-wide economic implications

Figure 25 shows that shipping decarbonisation affects not only the marine fuel mix, but also upstream fuel costs and energy-system investment. Panel (a) indicates that average shipping fuel prices rise in the near term across all decarbonisation pathways as clean-fuel supply chains scale up, but in the standard 1.5deg case they converge and fall slightly below BAU by 2100, implying long-run cost benefits from early hydrogen-based fuel deployment. The 1.5deg-IMO and 1.5deg-MEPC cases bring that transition forward, with fuel prices moving below the 1.5deg pathway already around mid-century. The clearest exception is 1.5deg-NA: excluding ammonia drives a sharp surge in average fuel prices, eventually to more than five times the reference level, because shipping is forced toward less scalable and more expensive alternatives while oil becomes increasingly penalised under the 1.5 °C constraint. This confirms that fuel availability matters more for long-run shipping cost than policy design alone.

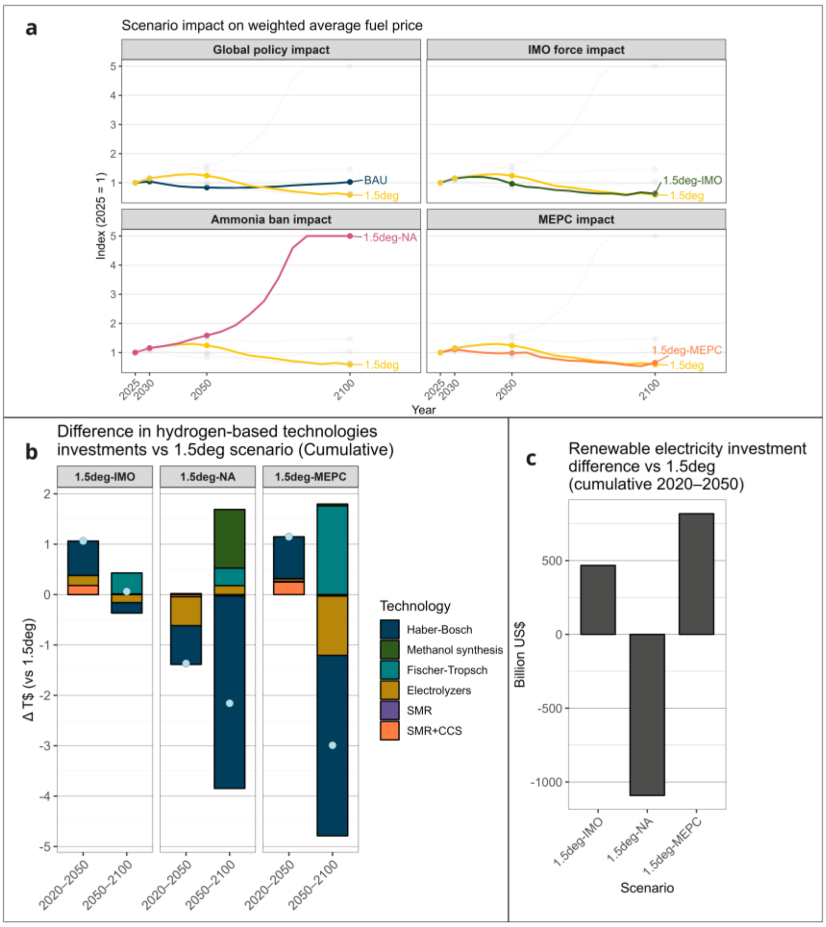

Figure 25: Scenario Cost Panel

Panel (b) shows the associated change in cumulative investment in hydrogen-based supply chains relative to the 1.5deg reference. The 1.5deg-IMO scenario requires additional mid-century spending, roughly split between green hydrogen and blue hydrogen supply and ammonia synthesis, to accelerate the transition. By contrast, 1.5deg-NA reduces cumulative hydrogen-chain investment because ammonia synthesis is largely avoided and the system shifts toward methanol and Fischer–Tropsch routes instead. The 1.5deg-MEPC case shows the strongest early build-out, with substantially higher investment before 2050, especially in blue hydrogen and Haber–Bosch capacity, followed by lower investment later in the century as mature supply chains reduce future capital needs.

Panel (c) shows the same logic from the electricity side. Relative to 1.5deg, 1.5deg-IMO requires moderately higher renewable electricity investment, while 1.5deg-NA requires much less because lower hydrogen production reduces demand for clean power. In contrast, 1.5deg-MEPC induces a large increase in renewable investment before 2050, driven by faster scale-up of green ammonia and other hydrogen-based fuels. Overall, the figure shows that shipping decarbonisation has visible system-wide consequences: earlier and stronger maritime action raises near-term investment needs, but helps lower long-run fuel costs and accelerates the build-out of hydrogen and renewable electricity supply chains.

Beyond shipping interactions

Figure 26 shows that shipping decarbonisation has visible spillovers into the rest of the energy system, but these spillovers are concentrated in a few sectors rather than being economy-wide everywhere. Panel (a) indicates that commercial/agriculture and residential emissions change very little across shipping scenarios, while the clearer differences appear in industry and other transport. In the baseline-based cases, shipping-specific policy draws biomass feedstock and biofuels toward international shipping, leaving slightly less availability for other transport modes and industry. Even so, all sectoral trajectories remain within the AR6 scenario ranges, which supports the internal consistency of the model. Panel (b) shows this biomass competition directly: road-transport biofuel use diverges most strongly between BAU and BAU-MEPC, and under 1.5deg-NA road biofuel use is also lower because banning ammonia pushes shipping to rely more heavily on biofuels.

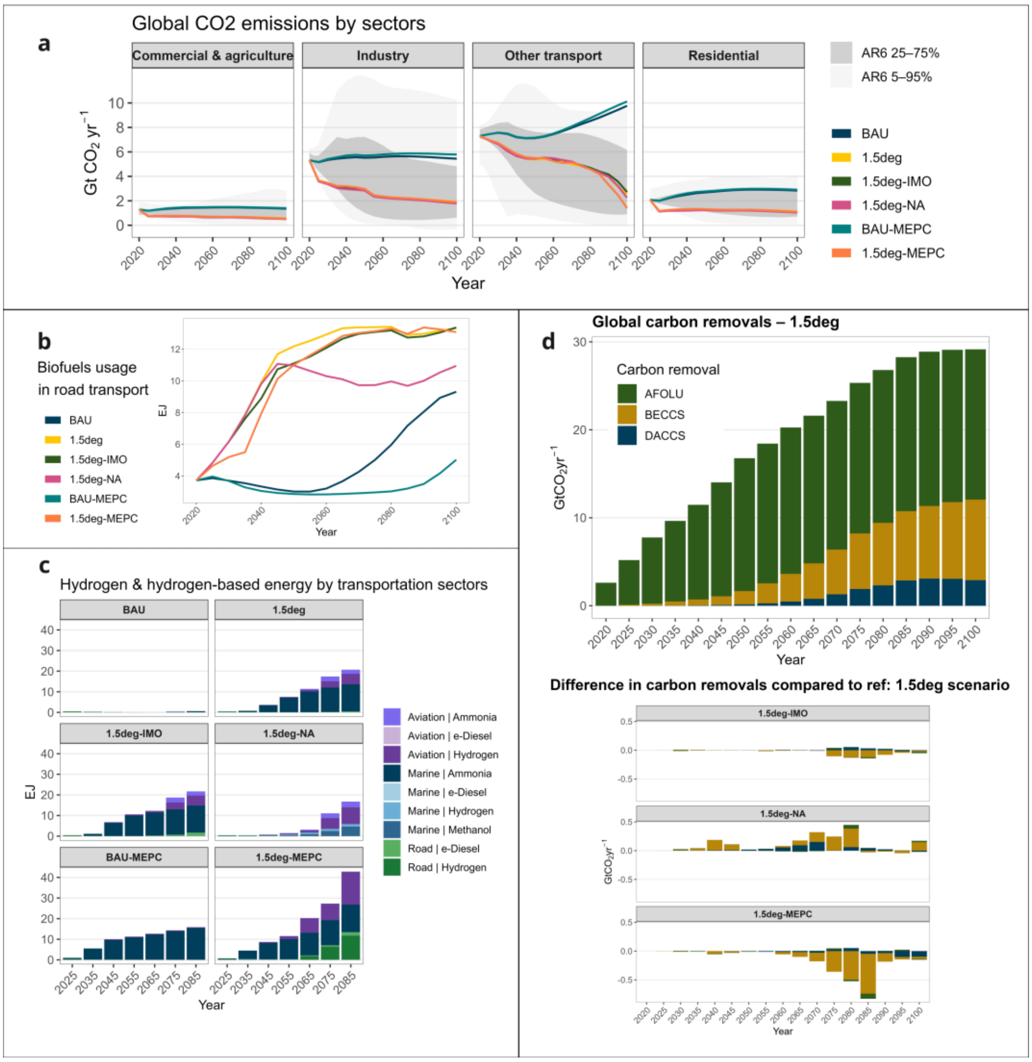

Figure 26: Sectoral Emission Panel

Panel (c) shows even stronger cross-sector coupling for hydrogen and hydrogen-based fuels. When ammonia is available, namely in 1.5deg, 1.5deg-IMO, and 1.5deg-MEPC, shipping absorbs most hydrogen in the form of ammonia. The 1.5deg-MEPC case stands out because earlier and stronger maritime policy accelerates ammonia production enough to lower upstream hydrogen costs and create spillovers into aviation and road transport by the end of the century. By contrast, in 1.5deg-NA, aviation becomes the dominant hydrogen user from mid-century onward, while shipping relies mainly on methanol and some marginal e-diesel instead. This again underlines that ammonia availability is central not only for shipping itself, but also for the distribution of hydrogen across sectors.

Panel (d) shows that these fuel shifts also affect the need for carbon removals. The upper panel reports the scale of AFOLU, BECCS, and DACCS removals in the reference 1.5deg pathway, while the lower panel shows deviations under alternative shipping scenarios. The 1.5deg-IMO case requires slightly lower removals later in the century, whereas 1.5deg-NA increases removals because the system relies more on carbon-dependent fuels and loses the most scalable zero-carbon marine option. The 1.5deg-MEPC pathway reduces removals most strongly in the later decades, consistent with earlier maritime decarbonisation easing pressure on the rest of the system. Overall, the figure shows that marine fuel choices affect not only shipping outcomes, but also biofuel allocation, hydrogen use in other transport sectors, and the scale of negative emissions required to meet long-term climate goals.

MEPC-timing sensitivity

Figure 27 isolates the effect of when the MEPC -style sectoral pricing starts, using the standard 1.5deg case as the reference. Panel (a) shows that earlier implementation shifts the cumulative fuel mix much more strongly away from oil and toward ammonia and, to a smaller extent, biofuels. When pricing starts in 2025, cumulative oil-based fuel use falls the most, by roughly 180 EJ relative to the 1.5deg reference, and this is offset mainly by a large increase in ammonia plus a more modest rise in biofuels. Delaying the start to 2030 or 2035 still reduces oil use, but the substitution toward ammonia becomes noticeably smaller. In other words, the later the policy begins, the less time the sector has to build low-carbon fuel chains and displace fossil fuel use over the century. This is consistent with the broader result that the timing of sectoral policy matters not only for emissions, but also for the scale and speed of ammonia deployment.

Panel (b) shows the same message in emissions terms. Relative to the 1.5deg reference, starting MEPC pricing in 2025 reduces cumulative shipping CO_2 emissions by about 16.9 $GtCO_2$ over 2020–2100, compared with about 8.0 $GtCO_2$ for a 2030 start and 5.9 $GtCO_2$ for a 2035 start. The effect is therefore large and highly time-sensitive: an earlier start roughly doubles or triples the cumulative emissions benefit compared with later implementation. This happens because earlier policy forces fuel switching while a larger share of lifetime fleet turnover is still ahead, allowing the sector to avoid lock-in to fossil-fuel vessels and to accelerate the build-out of ammonia-based supply chains.

Panel (c) adds an important system-wide perspective. Early action is not only more effective in reducing fuel use and emissions, but can also lower total policy cost relative to the 1.5 °C reference. In the figure, the 2025 MEPC start reduces cumulative policy cost by around 3%, whereas a 2030 start is close to neutral and a 2035 start slightly increases costs. This suggests that earlier shipping-sector action can reduce long-run system cost by inducing earlier investment in hydrogen and ammonia supply chains, which then lowers later fuel and mitigation costs. By contrast, late action sacrifices part of that benefit, because the system has less time to learn, scale, and substitute away from oil. This interpretation is fully aligned with the paper's broader finding that the 1.5°C-mepc pathway prioritises early build-out, especially in blue hydrogen and ammonia synthesis, and that these early investments reduce longer-term costs.

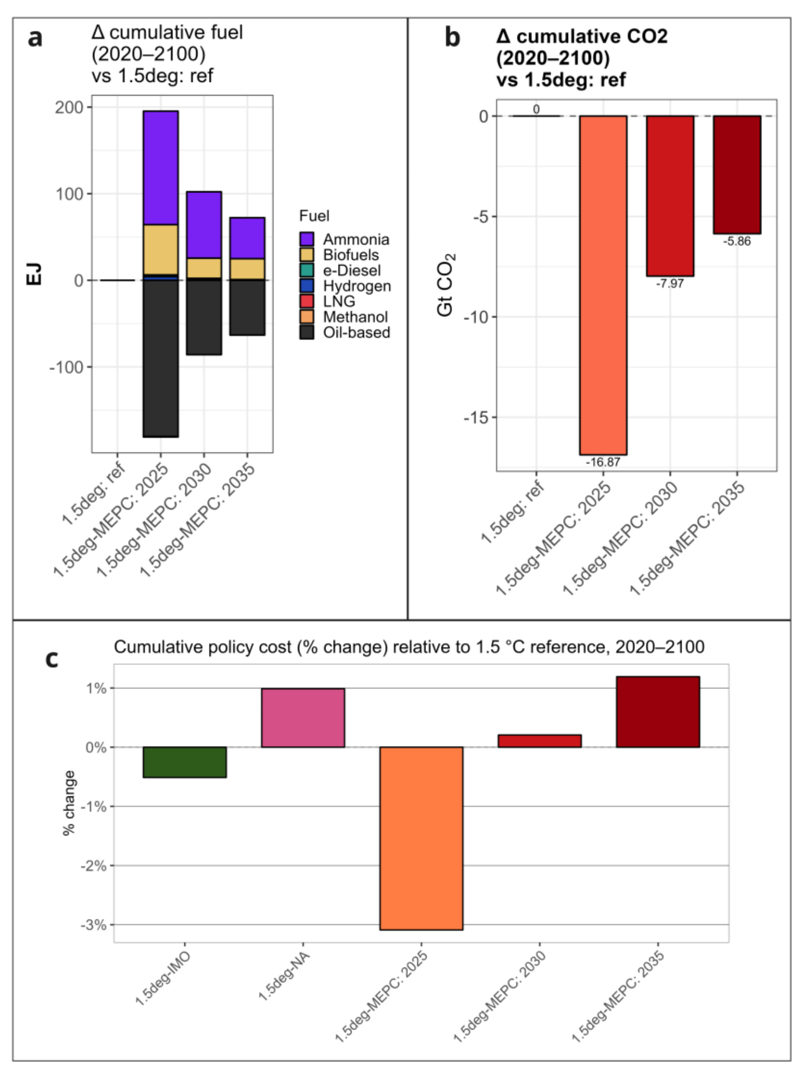

Figure 27: Panel with key Scenario Deltas

Taken together, the figure shows that MEPC-style sectoral policy is not only about stringency, but also about timing. Starting earlier produces a much larger cumulative shift away from oil, larger ammonia deployment, substantially lower century-scale CO_2 emissions, and lower overall policy cost. Delaying implementation weakens all of these effects. This reinforces one of the main conclusions of the modelling exercise: in shipping, where fleet turnover and fuel-infrastructure build-out are slow, policy timing is itself a major determinant of transition success.

4.2 TNO Opera National Model

Base Scenario

Introducing a higher spatial resolution for the Port of Rotterdam region results in material changes to the modelled energy system. Total final energy demand increases by 80 PJ, which is roughly 3% of national final energy use. The increase is concentrated in industry: industrial final energy demand rises by 37 PJ (7%), and feedstock demand increases by 32 PJ (13%). Overall, these differences indicate that explicitly representing spatial constraints and infrastructure linkages within the port area alters the model's optimal configuration of industrial production routes and associated energy and feedstock requirements.

Figure 28: aggregated national energy carrier production in 2030, 2040 and 2050 (PJ) forthe Base case without Port of Rotterdam regionalisation (top) and the PoR case with Port of Rotterdam regionalisation (bottom). Natural gas is shown separately from other fossil carriers due to its distinct system role. summarises the national energy carrier production levels for 2030, 2040, and 2050 under the two spatial configurations. The upper panel shows results for the Base configuration without explicit regionalisation of the Port of Rotterdam, while the lower panel shows results for the configuration with Port of Rotterdam regionalisation. Natural gas is reported separately from the other fossil carriers to reflect its distinct function within the system compared with the remaining fossil energy carriers.

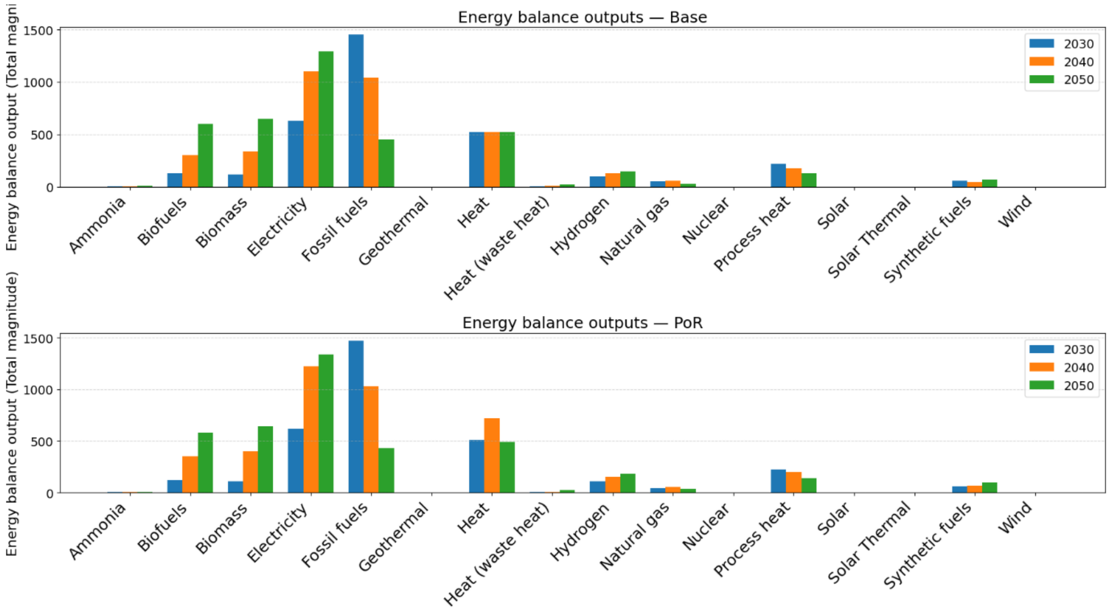

Figure 28: aggregated national energy carrier production in 2030, 2040 and 2050 (PJ) forthe Base case without Port of Rotterdam regionalisation (top) and the PoR case with Port of Rotterdam regionalisation (bottom). Natural gas is shown separately from other fossil carriers due to its distinct system role.

Overall, the results indicate that explicitly regionalising the Port of Rotterdam drives a structural change in the Netherlands' decarbonisation pathway. With higher spatial resolution, the model reveals stronger interdependencies between offshore wind expansion, hydrogen production, synthetic fuel synthesis, and industrial feedstock demand. At the same time, the higher-resolution representation shifts outcomes in the built environment towards decentralised electrification, particularly through greater reliance on electric heat pumps. These interactions are much less visible in lower-resolution national representations, which tend to smooth out infrastructure constraints and localised system couplings. The findings, therefore, underscore the value of explicitly modelling port-industrial clusters within integrated energy system analyses (Javanmardi et al., 2025).

Increasing the spatial resolution of the Port of Rotterdam leads to pronounced redistributions in where energy is produced, converted, and consumed across the Netherlands, while leaving overall system totals largely unchanged. Total electricity generation rises by about 4%, and electricity use increases by 52 PJ (4%), indicating that the main effect is spatial reallocation rather than a change in aggregate system scale. In other words, once port-level constraints and infrastructure interactions are represented explicitly, the model reorganises the geography of energy supply and demand.

Electricity

Electricity generation remains broadly stable in Mid NL and North NL, but several other regions show substantial changes. In 2050, generation decreases in South Holland by 43 PJ (22%), in North Brabant by 13 PJ (15%), and in Limburg by 9 PJ (10%). By contrast, generation increases in Zeeland by 10 PJ (51%), in North Holland by 13 PJ (15%), and—most strongly—in offshore regions by 102 PJ (17%). Notably, generation declines in South Holland (the region containing the Port of Rotterdam), while neighbouring provinces and offshore areas compensate for the reduction. The corresponding reallocations on the demand side are shown in Figure 29: Regional changes in energy carrier inputs (final consumption) between the Base and PoR cases in 2050 (PJ/yr). For comparability, the Port of Rotterdam sub-regions are combined with the remaining part of South Holland and reported jointly as "South Holland" (regional energy carrier inputs in 2050).

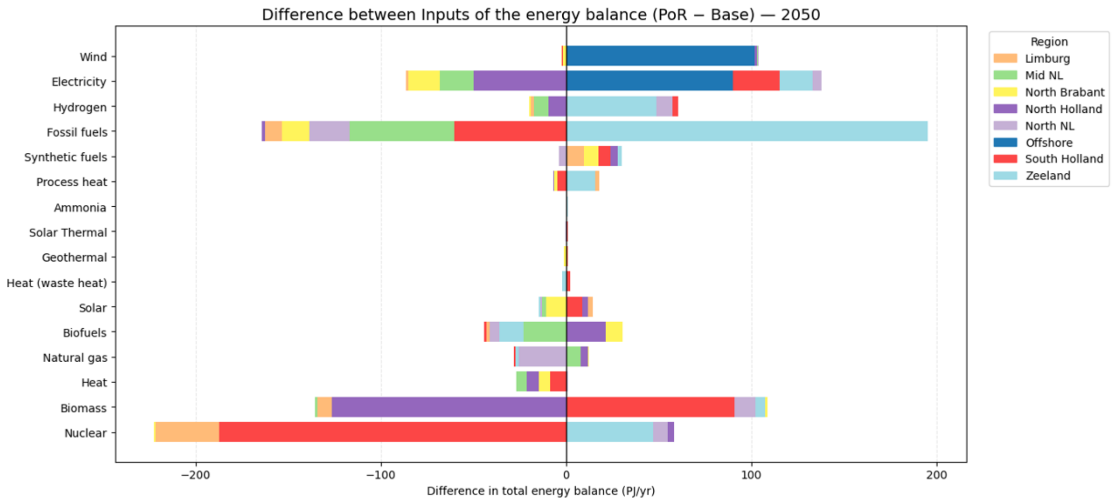

Figure 29: Regional changes in energy carrier inputs (final consumption) between the Base and PoR cases in 2050 (PJ/yr). For comparability, the Port of Rotterdam sub-regions are combined with the remaining part of South Holland and reported jointly as "South Holland"

Electricity consumption in offshore regions increases by 90 PJ (75%), driven by the expansion of offshore electrolytic hydrogen production. Demand also rises by 25 PJ (11%) in South Holland and by 18 PJ (24%) in Zeeland. By contrast, electricity consumption declines by 50 PJ (21%) in North Holland, by 17 PJ (11%) in North Brabant, and by 18 PJ (8%) in Mid NL, while remaining broadly stable in Limburg and North NL. Overall, these shifts align with the relocation of hydrogen production, with electricity increasingly directed to electrolysis in offshore and coastal regions. South Holland is a notable exception: there, higher electricity use is mainly attributable to greater direct electrification of industrial processes, particularly in the Port of Rotterdam's chemical sector.

Hydrogen

When the Port of Rotterdam is represented at higher spatial resolution, national hydrogen production increases by 41 PJ (30%). In the lower-resolution configuration, a substantial share of hydrogen production is allocated to South Holland. After introducing detailed regionalisation, however, hydrogen production in South Holland falls by 45 PJ (90%), while offshore hydrogen production increases by 61 PJ. Output in Zeeland also rises by 20 PJ, consistent with the broader spatial shift observed for electricity generation. By 2050, hydrogen production becomes strongly offshore-oriented: offshore electrolysis supplies 123 PJ, corresponding to 67% of total national hydrogen production.

Hydrogen demand increases in parallel, rising by 41 PJ (32%) at the national level. The additional consumption is concentrated in Zeeland and North NL, while hydrogen use declines in North Holland and Mid NL. Overall, the results point to an increasing spatial decoupling between hydrogen production and end use: hydrogen is progressively produced offshore and in coastal regions, while consumption remains concentrated in industrial centres and fuel-conversion hubs located elsewhere.

Bio and Synthetic fuels

Biofuel production shows a moderate but clearly identifiable spatial shift. Zeeland remains the main production region, reaching 235 PJ in 2050 and increasing slightly relative to the lower-resolution case. Biofuel output in South Holland increases by 74 PJ, while production in North Holland is largely displaced. In contrast, national biofuel consumption decreases by 20 PJ (4%). North Holland is a notable exception, where biofuel consumption rises, driven by higher biokerosene demand in aviation.

The most pronounced spatial response occurs for synthetic fuels. When the Port of Rotterdam is regionalised explicitly, national synthetic fuel production increases by 52 PJ (65%). Most of this increase is located in South Holland, where production is close to three times higher by 2050, and in Zeeland, where production roughly doubles. Synthetic fuel demand increases in parallel, with the largest rise occurring in the Port of Rotterdam area.

Alternative Scenarios

Four alternative futures are analysed to test how sensitive the Dutch energy system, and in particular the role of the Port of Rotterdam (PoR), is to a set of strategic uncertainties. The scenario variants capture (i) the option to import renewable fuels, (ii) the introduction of a regional net-zero constraint for the PoR, (iii) the exclusion of nuclear deployment within the port region, and (iv) a nuclear pathway in which deployment is restricted to small modular reactors (SMRs). National-level deviations from the PoR reference case are summarised in Figure 30: Aggregated national-level changes in energy carrier balances relative to the PoR reference case. and Figure 31

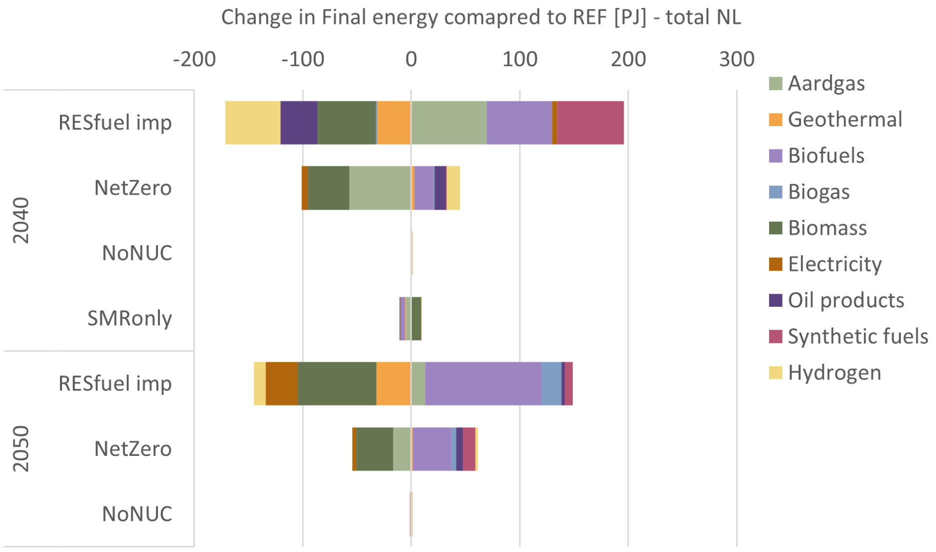

Figure 30: Aggregated national-level changes in energy carrier balances relative to the PoR reference case.

RES fuel import

Allowing renewable fuel imports leads to marked changes in both the national system configuration and the Port of Rotterdam's role. Access to imported, pre-processed fuels reduces the need for domestic low-carbon fuel production, which in turn lowers biomass import requirements, domestic biofuel production, domestic hydrogen output, and the associated offshore wind generation needed to supply electrolysis and conversion processes. Within the Port of Rotterdam, biomass inflows decline, most notably at Europoort, and both synthetic fuel and biofuel production decrease as imported renewable fuels increasingly displace domestic conversion activities.

Net-zero Port of Rotterdam

Adding a net-zero GHG constraint for the Port of Rotterdam, on top of the national net-zero target, mainly affects fossil fuel use and refinery operations. At the national level, natural gas imports decrease, and the reduced reliance on fossil generation is compensated primarily by higher offshore wind deployment, which partly displaces nuclear generation. Within the port region, the stricter constraint accelerates the transition away from fossil-based refining and leads to a marked increase in biofuel production coupled with CCS, particularly in Europoort.

No nuclear in the Port of Rotterdam

Prohibiting nuclear deployment within the Port of Rotterdam has only a marginal effect on the national energy system. Any foregone capacity is largely reallocated to other regions—most notably Zeeland—without causing meaningful changes in overall system balances.

SMR-only nuclear in the Port of Rotterdam

When large-scale nuclear plants are disallowed in the Port of Rotterdam but small modular reactors (SMRs) remain an option, total nuclear generation declines slightly. Within the port area, SMRs are primarily sited in Pernis and operate mainly as exporters, supplying electricity and heat to other PoR sub-regions.

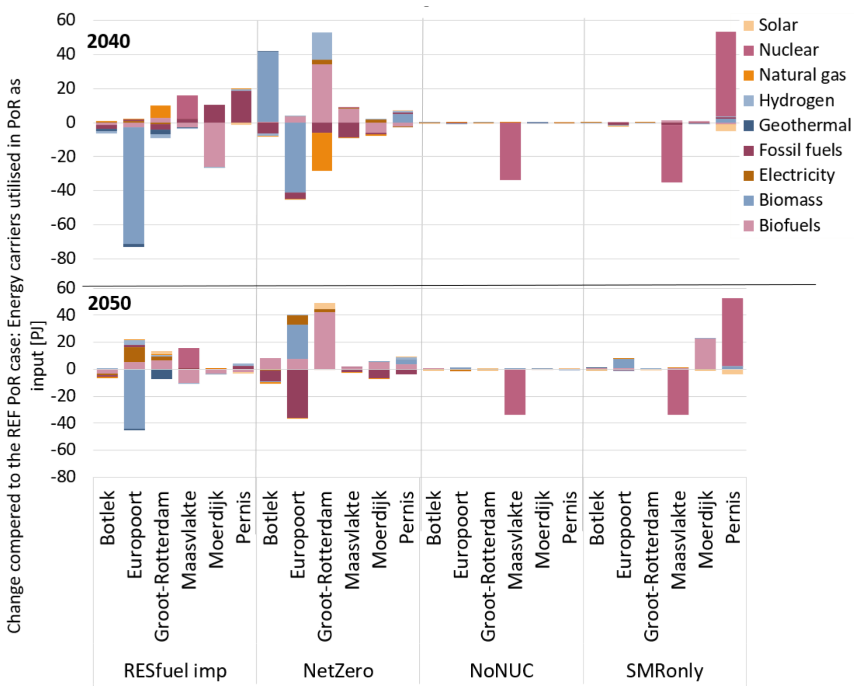

Figure 31: Port of Rotterdam sub-regional changes in energy carrier consumption (PJ) relative to the PoR reference case: 2040 (top) and 2050 (bottom).

Discussion

The results underscore the central role of large port–industrial regions in national energy transitions and show that their system behaviour is difficult to represent credibly without high spatial resolution. Ports such as the Port of Rotterdam combine multiple critical functions within a relatively small area: they serve as entry points for energy and material imports; host concentrated industrial activity and refineries; sit close to offshore assets such as wind farms, electrolysers, and CO_2 storage; and border densely populated urban areas with substantial residential and service-sector demand. This tight co-location of energy-intensive industry, logistics, conversion infrastructure, and urban load makes port regions structurally distinct from most other parts of the energy system (Damman et al., 2025).

The modelling outcomes indicate that making this complexity explicit can materially change system results. When the Port of Rotterdam is represented as a regionalised cluster, structural patterns emerge that are largely smoothed out in a lower-resolution national representation. A key outcome is the functional differentiation between offshore regions, which specialise in electricity generation and hydrogen production, and the port region, which concentrates on downstream conversion, fuel synthesis, and industrial demand. This aligns with broader findings that spatial aggregation can hide infrastructure constraints and bias the modelled location of technologies and conversion processes (Javanmardi et al., 2025).

The transformation within the port itself is particularly pronounced. In 2030, the port remains predominantly fossil-based, importing and using roughly 1,600 PJ of fossil energy. By 2050, fossil imports fall to about 400 PJ, while biomass imports rise to more than 660 PJ and are increasingly converted into biofuels coupled with carbon capture. At the same time, the port becomes the dominant national centre for synthetic fuel production, while depending heavily on electricity and hydrogen produced mainly offshore and in neighbouring regions. This reflects a fundamental redefinition of the port's function: **from a fossil-fuel import and refining hub to a low-carbon fuel-conversion hub, with biofuels and synthetic fuels as core outputs.**

From a spatial perspective, this shift has direct implications for infrastructure needs. Biomass, biofuels, and synthetic fuels differ from fossil fuels in volumetric energy density and handling characteristics, which translates into different storage footprints and higher logistics intensity for comparable delivered energy services (Sornn-Friese, 2024). In addition, synthetic fuel production introduces additional infrastructure requirements for hydrogen handling and for CO_2 supply, transport, and management, increasing both spatial and operational complexity in port areas that are already highly space-constrained (Damman et al., 2025). These elements are not represented as explicit physical constraints in the current optimisation and should therefore be evaluated in follow-up spatial feasibility and siting analyses.

The alternative scenarios provide further evidence of the sensitivity of these spatial outcomes to strategic choices. Allowing large-scale imports of renewable fuels reduces the need for domestic conversion capacity, associated offshore wind build-out, and hydrogen production, and it lowers biomass inflows and local conversion activity within the port. **This implies that renewable fuel trade can ease local spatial constraints, but at the cost of greater dependence on international supply chains.** Based on the WITCH IAM results, most fuels will be produced outside Europa, as electricity is cheaper there, though at the moment the EU and China do lead the solar and wind power development.

By contrast, imposing a net-zero GHG constraint specifically on the Port of Rotterdam strengthens its position as a biofuel production and carbon capture hub, particularly in Europoort. This highlights a practical trade-off between regional climate ambition and spatial feasibility in ports where land-use and infrastructure siting constraints can become binding (Javanmardi et al., 2025).

Finally, the limited system response to whether nuclear is included or excluded within the port suggests that **nuclear siting in the PoR is secondary relative to choices on renewables deployment, renewable fuel imports, and industrial conversion pathways.** From a policy standpoint, the results support prioritising integrated planning of offshore wind, hydrogen, and CO_2 infrastructure in conjunction with port conversion capacity and industrial demand, consistent with ports-as-hubs perspectives (Damman et al., 2025; Sornn-Friese, 2024).

5. Discussion and conclusions

The goal of T3.6 was to integrate T3.1-3.5 to supply a long-term (2030-2050) assessment of energy demands and availability under various growth scenarios. Integrating the effect of new energy mediums on operations, bunkering strategies, identifying key infrastructure and fuel acceptance by modalities. Relates to WP7 and WP9. As can be seen in Section 3.4, this is not a straightforward exercise and requires significant effort. Especially as in many cases, models that were already (partially) developed have been adapted to meet the goals of MAGPIE. However, despite the effort and coordination, the output is improved as we can now study a consistent future for decarbonisation. For the smaller models, the effort is smaller, as in many cases a scenario was identified and used; this scenario could easily be replaced by other scenarios, as this is, by nature, the goal of these smaller models (to study the impact of scenarios in a detailed manner).

With the models created under T3.6 and applied in T3.2-3.5, the long term assessment at various detail levels has been achieved. Furthermore, the models, could be used for the assessment of demonstrator scale-up, provided sufficient data is available.

The integration/cascading of results was done and led to interesting insights, as shown in part in Chapter 4. A key takeaway for MAGPIE is that, despite the serious downsides of Ammonia as a fuel, the models demonstrate that bio-fuel alternatives will fall short and the import scenarios required to meet the EU energy demand lead to economic stagnation and globally to much higher energy cost levels. In Opera Nuclear (SMR) is considered as well, but the input is secondary to import choices and potential and requires quick adaptation to be successful. Furthermore, OPERA confirms that a large industrial complex, like the Port of Rotterdam, would play a key role in energy provision and security.

On the policy level this leads to two important recommendations:

1. To lower the costs of energy and investments in energy, ammonia requires serious consideration, a world of energy without is possible, but again the costs of energy will be far larger than with ammonia as a carrier and fuel.
2. SMR/Nuclear is to be considered (and supported) soon to be relevant based on the model outcomes. As these do not yet include the current global turmoil, energy independence was not yet a key consideration, however, this further strengthens the need for alternative power sources

It should be noted that for ammonia, little is known about the large scale application and the indirect GHG potential. In the past LNG was seen as a key fuel, until methane slip offset the GHG balance in combination with a price shock. Similarly Ammonia slip could indirectly lead to N_2O forming, leading to additional GHGs in the atmosphere. As not enough is known about the potential slip and counter measures, it is key for Policy to addresses these gaps soon before, like LNG, serious commitments are made..

Finally the results of T3.6 can be used further in T3.2-T3.5 as well as WP7, WP8 and WP9. As such we see a successful completion of T3.6.

6. References

Brändle, G., Schönfisch, M., Schulte, S., 2021. Estimating long-term global supply costs for low-carbon hydrogen. Applied Energy 302, 117481. doi:10.1016/j.apenergy.2021.117481.

Bosch, J., Staffell, I., Hawkes, A.D., 2017. Temporally-explicit and spatially-resolved global onshore wind energy potentials. Energy 131, 207–217. doi:10.1016/j.energy.2017.05.052.

Bosch, J., Staffell, I., Hawkes, A.D., 2018. Temporally explicit and spatially resolved global offshore wind energy potentials. Energy 163, 766–781. doi:10.1016/j.energy.2018.08.153.

Couper, J.R., Hertz, D.W., Smith, F.L., 2007. Process economics, in: Green, D.W., Perry, R.H. (Eds.), Perry's Chemical Engineers' Handbook (8th Edition). McGraw-Hill Professional Publishing, Blacklick, USA

Damman, S., Wardeberg, M., & Gabrielii, C. (2025). Policies shaping energy transitions in ports and harbours: A "whole systems" perspective from Norway. Energy Research & Social Science, 125, 104101. https://doi.org/10.1016/j.erss.2025.104101

Damodaran, A., 2025. Country default spreads and risk premiums. Web Page. Accessed at 18.09.2025 at https://pages.stern.nyu.edu/~adamodar/New_Home_Page/datafile/ctryprem.html.

DNV, 2024. Energy transition outlook 2024. URL: https://www.dnv.com/publications/energy-transition-outlook-2024/.

ElaadNL. (n.d.). From Charging Profile Generator: https://charging.elaad.nl/

Elberry, A. M., Scheepers, M., van Stralen, J., Giraldo, J. S., & van der Zwaan, B. (2025). Decarbonizing the Dutch industrial sector: between maintaining domestic production and partial relocation. Energy and Climate Change, 100205.

Electric Power Research Institute. (2022). Adequacy Standards & Criteria. From https://gridops.epri.com/Adequacy/standards

Energie Opwek Nederland. (2025). From https://energieopwek.nl/

Gobal-Solar-Atlas, 2024. Gobal solar atlas. URL: https://globalsolaratlas.info/.

Gobal-Wind-Atlas, 2024. Gobal wind atlas. URL: https://globalwindatlas.info/. RENA. (2022). Unlocking the Potential of Distributed Energy Resources: Power system opportunities and best practices.

Javanmardi, K., van der Hilst, F., Fattahi, A., Ramirez Camargo, L., & Faaij, A. (2025). Unraveling the spatial complexity of national energy system models: A systematic review. *Renewable and Sustainable Energy Reviews, 213*, 115470. https://doi.org/10.1016/j.rser.2025.115470

IEA. (2024). Netherlands 2024: Energy Policy Review.

ILO, I.L.O., 2025. Ilostat data explorer – mean nominal hourly labour cost per employee by economic activity. URL: https://rshiny.ilo.org/dataexplorer00.

IRENA. (2022). Unlocking the Potential of Distributed Energy Resources: Power system opportunities and best practices.

Moritz, M., Schönfisch, M., Schulte, S., 2023. Estimating global production and supply costs for green hydrogen and hydrogen-based green energy commodities. International Journal of Hydrogen Energy 48, 9139–9154. doi:10.1016/j.ijhydene.2022.12.046.

Naghash, H. (2026). *Beyond Sectoral Thinking: International Shipping Fuels in an Energy-Economy System,* Doctoral Thesis https://doi.org/10.4233/uuid:cbf4be86-357e-42a3-ab85-c2b36281d3e3

Netbeheer Nederland. (2023). Het energiesysteem van de toekomst: de II3050-scenario's.

PBL Netherlands Environmental Assessment Agency. (n.d.). *MIDDEN: Manufacturing Industry Decarbonisation Data Exchange Network*. Retrieved January 31, 2026, from https://www.pbl.nl/en/middenweb

Peters, M.S., Timmerhaus, Klaus D., 1991. Plant design and economics for chemical engineers. International 2 revised ed ed., McGraw-Hill Education (ISE Editions).

Pietzcker, R.C., Stetter, D., Manger, S., Luderer, G., 2014. Using the sun to decarbonize the power sector: The economic potential of photovoltaics and concentrating solar power. Applied Energy 135, 704–720. doi:10.1016/j.apenergy.2014.08.011.

Port of Rotterdam. (n.d.). Energy and electricity. From https://www.portofrotterdam.com/en/setting/industry-port/energy-and-electricit

Port of Rotterdam. (n.d.). Charging station for electric trucks. From https://www.portofrotterdam.com/en/port-future/energy-transition/making-logistics-chains-more-sustainable/charging-station-for

Punt, L., Ghiassi-Farrokhfal, Y., & Loke, G. G. (2024). Operationalizing smart charging: A robust optimization interpretation of flexibility vs uncertainty. Available at SSRN.

Scheepers, M., Palacios, S. G., Jegu, E., Nogueira, L. P., Rutten, L., van Stralen, J., Smekens, K., West, K., & van der Zwaan, B. (2022). Towards a climate-neutral energy system in the Netherlands. *Renewable and Sustainable Energy Reviews, 158*, Article 112097. https://doi.org/10.1016/j.rser.2022.112097

Sornn-Friese, H. (2024). *Ports as energy transition hubs: An exploratory study*. CBS Maritime. Retrieved January 31, 2026, from https://research.cbs.dk/en/publications/ports-as-energy-transition-hubs-an-exploratory-study/

van Stralen, J. N., Dalla Longa, F., Daniëls, B. W., Smekens, K. E., & van der Zwaan, B. (2021). Opera: a new high-resolution energy system model for sector integration research. Environmental Modelling & Assessment, 26, 873-889. doi.org/10.1007/s10666-020-09741-7.

Statistics Netherlands. (2025, July 9). *Population dynamics; birth, death and migration per region* [Data set]. Retrieved January 31, 2026, from https://www.cbs.nl/en-gb/figures/detail/37259eng

TNO. (2024). Towards a sustainable energy system for the Netherlands in 2050.

WITCHmodel(2026) https://www.witchmodel.org/model/ (visited 14-05-2026)

Annex 1: Thesis to

PhD Linda Punt: https://pure.eur.nl/en/publications/flexibility-and-uncertainty-in-power-systems-insights-from-electr/

PhD Hesam Nagash, Data DOI

10.4121/6096001e-660c-429e-a581-8855bec9b97f.v1